MIXING BY AGITATION OF MISCIBLE LIQUIDS

PROEFSCHRIFT

TER VERKRIJGING VAN DE GRAAD VAN DOCTOR IN DE TECHNISCHE WETENSCHAP AAN DE TECHNISCHE HOGESCHOOL TE DELFT, OP GEZAG VAN DE RECTOR MAGNIFICUS Dr. O. BOTTEMA, HOOGLERAAR IN DE AFDELING DER ALGEMENE WETENSCHAPPEN, VOOR EEN COMMISSIE UIT DE SENAAT TE VERDEDIGEN OP WOENSDAG 16 DECEMBER 1953, DES NAMIDDAGS TE 2 UUR

DOOR

JAN GERRIT VAN DE VUSSE

NATUURKUNDIG INGENIEUR

GEBOREN TE ROTTERDAM

UITGEVERIJ EXCELSIOR — 's-GRAVENHAGE

PROMOTOR: PROF.IR H.KRAMERS

AAN MIJN VROUW

CONTENTS

	Page
Summary	7
1. *Introduction*	9
1.1. Definitions	9
1.2. Brief survey of the literature	10
1.2.1. Mixing criteria	10
1.2.2. Power consumption	10
1.3. Different types of agitators and their flow pattern	12
1.4. Scope of the present investigation	
2. *Apparatus and measuring technique*	14
2.1. Mixing time	14
2.2. Determination of the power consumption	16
3. *The mixing performance of the cone stirrer*	17
3.1. Pumping action	17
3.2. Mixing time	19
3.2.1. Experiments	19
3.2.2. Theory and calculations	20
3.2.3. Comparison of the theory with the experimental results	26
3.3. Power consumption	27
3.3.1. Experiments	27
3.3.2. Calculations	28
3.3.3. Comparison of the theory with the experimental results	28
3.4. Mixing energy	29
4. *Mixing performance of paddle stirrers, propeller stirrers and turbomixers*	31
4.1. Mixing time	31
4.1.1. Dimensional considerations	31
4.1.2. Influence of the density Froude number	33
4.1.3. The influence of Reynolds' number	34
4.1.4. Influence of dimensions of vessel relative to stirrer dimensions	34
4.1.5. Influence of the location of the stirrer, etc.	35

Page

4.2. Pumping capacity 36
4.2.1. Paddle stirrers and turbomixers 36
4.2.2. Paddle stirrer with inclined blades 39
4.2.3. Propeller stirrers 42
4.2.4. Recapitulation 43
4.3. Vortex formation 44
4.4. Rules for scaling up 44
4.5. Power consumption 45

5. *Discussion of optimum stirring conditions* 48
5.1. Conditions for optimum performance 48
5.2. Influence of liquid volume to be mixed 49
5.3. Influence of stirrer and vessel dimensions 49
5.3.1. Influence of the stirrer/vessel diameter ratio $\frac{d}{D}$ 49
5.3.2. Influence of liquid height $\frac{H}{D}$ 51
5.3.3. Width of stirrer blade 51
5.4. Type of the stirrer 52
5.4.1. Influence of blade angle α 52
5.4.2. Influence of vane angle β 53
5.5. Comparison with jet mixing 53
5.6. Comparison with the cone stirrer 54
5.7. Concluding remarks 54

6. *Continuous mixing of liquids* 55
6.1. Introduction 55
6.2. Measurements (mixing times) 56

List of symbols 58

References 60

Addendum: Tables and figures

SUMMARY

The performance of several types of agitators has been assessed for the mixing of miscible liquids in batch operation.

The time, necessary to homogenize two superimposed layers of miscible liquids was measured. An optical technique, known as the "Schlieren" method, was used to determine the moment at which uniformity is reached. Besides, the power consumption of the stirrers was measured. The influence of liquid properties and of the conditions of agitation was investigated and could be explained.

From the results relations containing dimensionless groups were derived, both for the mixing time and for the power consumption.

An important result of this study is the discovery that in the region of turbulent flow the mixing time is related to the pumping capacity of the stirrer. The mixing time appears to be approximately proportional to the time required to circulate the liquid once, this time being equal to the ratio between the liquid volume and the pumping capacity of the stirrer.

General rules for the optimum shape and dimensions of the stirrers were derived from the relations for mixing time and power consumption.

Some experiments have been carried out on the steady-state mixing (continuous mixing) of liquids. The results found in the batch experiments could also be applied in this case.

1. INTRODUCTION

1.1. Definitions

By "mixing" will be meant any operation by means of which a non-uniform system is changed into a uniform one.

An amount of matter may be called uniform or homogeneous when the composition of an element of volume of appropriate size does not deviate by more than a fixed amount from the average composition of the entire system.

The mixing operation may form part of various chemical and physical processes, such as blending, dissolving, emulsification, heat transfer, chemical reactions etc.

In chemical engineering it is recognized as one of the "unit operations" and enjoys an increasing interest in literature. In spite of its importance, the mixing operation is in most cases still an "art" and the design of agitators and mixing vessels is based largely on experience.

The means of mixing are numerous; they are highly dependent on the purpose of the mixing and the nature of the substances to be mixed. This can be illustrated as follows:

Analysis of mixing

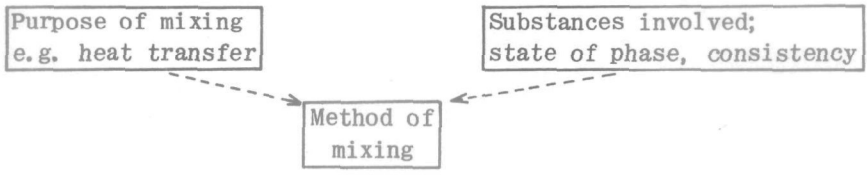

As to the nature of the substances to be mixed, the state of phase greatly influences the choice of the mixing method. The mixing operation can be classified according to the various possible combinations between the phases: gas, liquid and solid. By liquid-liquid mixing, for instance, will be meant the mixing of two miscible or immiscible liquids.

Important methods of mixing are: flow mixing, e.g. circulation by pumping, injection; vibrational mixing, e.g. by ultrasonics; mixing by rotating agitators.

In mixing two phenomena can be distinguished: a splitting up of the elements of volume and an interchange of the elements of volume.

In several cases e.g. in mixing miscible liquids, the molecular diffusion also contributes to the ultimate homogeneity of the system to be mixed. In practice, the exchange by molecular diffusion is negligible compared with the eddy diffusion due to the turbulence in the agitated system; it is only important when considering elements of volume of molecular dimensions.

1.2. Brief survey of the literature

1.2.1. *Mixing criteria*

Investigations on mixing are always based on a mixing criterion, which permits an evaluation of the stirring process. As a rule, the choice of criteria depends on the systems to be mixed, together with the purpose of the operation. Thus the following quantities have been used as mixing criteria.

a. Rate of solution and melting of solids in liquids (14, 27).
b. Rate of mass transfer in liquid-liquid extraction (16).
c. Rate of heat transfer (4, 20, 23).
d. Time required to produce a uniform mixture of two miscible liquids (1, 5, 21, 22, 29).
e. Velocity of reactions between two reacting liquids (2, 19, 30).
f. Other mixing problems and mixing criteria examined are the uniformity of suspensions (15, 39, 40, 31); the pumping capacity of the agitators (25, 32); the adsorption of a pigment on a suspended solid (13); and the corrosive action of liquids on metal surfaces (9, 12).

In all these criteria one or more of the elements: mass transfer, heat transfer and hydrodynamic behaviour can be recognized. Only with criteria a and c have satisfactory correlations been found. Most of the experiments described in the above-mentioned literature have been carried out in batch operations and only few concrete results have been published on the mixing of continuously flowing liquids (6).

1.2.2. *Power consumption*

In the literature much attention has been paid to the power consumption of rotating stirrers. It is not a mixing criterion in the true sense of the word and is difficult to correlate with practical quality data, such as the rate of solution, heat transfer, etc. For the design of the stirrer drive and for the knowledge of stirrer efficiency the power consumption is of great importance. Many experiments have been carried out to determine the

influence of rotor speed, dimensions of stirrer and vessel and physical properties of the liquid, on power consumption.

The measured power consumption P is included in a dimensionless group $\frac{P}{\rho n^3 d^5}$, which in most publications is plotted against a Reynolds' number ($Re = \frac{\rho n d^2}{\mu}$) (32).

This can be made plausible as follows: When Newton's law, which gives the resistance of a body in a flowing medium, is applied to the rotating agitator, the frictional resistance of the agitator in the liquid is: $F = c\ A\ \frac{1}{2}\ \rho v^2$, where the projected area of the stirrer in the direction of flow $A \sim d^2$ and $v \sim nd$. The dimensionless coefficient c is still a function of the condition of flow (Reynolds' number), type of stirrer, etc. The power consumption $P = F.v \sim \rho n^3 d^5$.

When vortex formation occurs, the dimensionless power consumption is also a function of Froude's number ($\frac{n^2 d}{g}$).

For all types of agitators it appears that in the "laminar" region ($Re < 200$), $\frac{P}{\rho n^3 d^5} = 120\ Re^{-1}$. In the turbulent region each type of agitator depends in a different way on Re. In the case of paddle stirrers $\frac{P}{\rho n^3 d^5}$ is about proportional to $Re^{-1/3}$, for propeller stirrers and turboximers it is about proportional to $Re^{-1/5}$ or even independent of Re. The latter is always the case when baffles have been placed in the mixing vessel (24).

A question often encountered in chemical engineering is, what rules must be used for scaling up of the apparatus, in order to obtain similar results in vessels of different dimensions.

As the dimensions of stirrer and vessel are usually enlarged geometrically, the scaling-up rule should give a relation between the number of revolutions required and a length dimension of the mixing device.

In actual practice a choice is made from the following rules: The power consumption per unit of liquid volume is kept constant, hence the product $n^3 d^2$ = constant.

The Reynolds' number is kept constant, giving nd^2 = constant.

The Froude number is kept constant, so that $n^2 d$ = constant.

The peripheral speed of the stirrer is kept constant, that is nd = constant.

Investigations by Hixson and others (14) show that the rules for scaling up derived from experimental results are dependent on the criterion applied, on the type of stirrer, the system to be mixed and the Reynolds' number at which mixing takes place.

1.3. Different types of agitators and their flow pattern

Mixing by agitation of liquids is caused by the transfer of momentum from the moving stirrer to the liquid. According to the way in which this occurs, stirrers may be divided into two categories:

a. The momentum is transferred by *shearing stresses*, i.e. the transfer is perpendicular to the direction of flow. This category includes the cone stirred, the bulb agitator, the rotating disc and others.
b. The momentum is transferred by *normal stresses*, i.e. the transfer is in the direction of flow. This category includes the paddle stirrer, the turbomixer and the propeller (fig. 2).

The latter three may in their turn be regarded as representatives of types distinguished according to flow pattern. We may distinguish three principal possibilities of flow, connected with the three axes of the coordinate system:

Tangential flow. This is found with all normal rotating stirrers, if no baffles or deflecting blades are present and the stirrer is placed centrally.

Axial flow. This is found with propeller type agitators.

Radial flow. This is found with turbine type stirrers (often fitted with deflecting blades) and to a certain extent with paddle stirrers.

As tangential flow does not contribute to the mixing in a vertical direction, this flow is not particularly desirable. Later it will be shown that tangential flow is always converted into radial flow by the centrifugal forces. This conversion can be promoted by baffling. In this way a "top-to-bottom" mixing is acquired, as in the case of an axial and a radial flow pattern.

1.4. Scope of the present investigation

The present investigation is devoted to the mixing of miscible liquids. For this system the mixing time proves to be an attractive criterion. In addition to the mixing time, the power consumption under various stirring conditions is measured. By comparing the mixing times and power consumptions of the various agitators conclusions are drawn as to their efficiencies.

All the agitators dealt with belong to the rotating type. As representative of the stirrers of category 1.3.a the cone stirrer is investigated (fig. 1). The paddle stirrer, the turbomixer and the propeller are studied as the most important representatives of the stirrers of category 1.3.b (fig. 2).

Most of the experiments were carried out in a 2-litre vessel (diameter and height about 14 cm) and with stirrers of about 6 cm diameter. The largest vessel used has a content of 45 litres (diameter and height about 38 cm) and the largest stirrer has a diameter of 16 cm.

2. APPARATUS AND MEASURING TECHNIQUE

2.1. Mixing time

The mixing time was determined by what is known as the "Schlieren" method. The arrangement is represented schematically in fig. 3. It is a modification of the arrangement used by TOEPLER (34). In order to avoid refraction the cylindrical mixing vessel was placed in a vessel with plane-parallel walls. Optical inhomogeneities in tne liquid contained in the mixing vessel, in the form of gradients in refractive indices, may produce "Schlieren", whereas absence of the latter indicates homogeneity of the liquid mixture.

In these experiments we started from a condition in which the two liquids were present as two superimposed layers. If the liquids are carefully introduced into the vessel, the interface can be clearly distinguished.

The following liquids were used:
water and dilute solutions of acetic acid in water;
water and dilute solutions of glycerin in water.

The mixing time was determined by taking as the starting point the moment at which the stirrer starts mixing and as the end point the moment of disappearance of the "Schlieren". As to the reliability of the "Schlieren" method for determining the mixing time, the following may be noted.

It is clear that the refractive index or the difference in refractive index has no influence on the time required to homogenize the two liquids. As stated above the "Schlieren" method is based on the fact that rays of light are deflected owing to refractive index gradients in the mixing vessel. It is therefore conceivable that the difference in refractive index influences the determination of the mixing time. It has been found experimentally, however, that only the "intensity" of the "Schlieren" is influenced by this difference.

The mixing time proves to be independent of the difference in refractive index, as is shown by fig. 4, where measurements at a given difference in density give about the same mixing time irrespective of the difference in refractive index.

This phenomenon is in agreement with the observation that the intensity of the striae does not vary greatly during the mixing process until a sudden decrease at the end of the experiment (see figure).

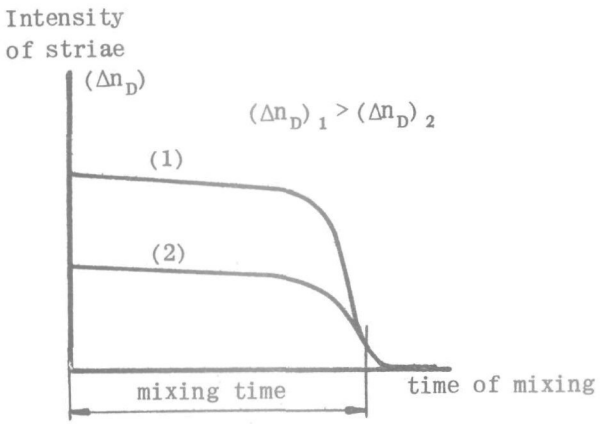

This behaviour can be explained by a study of the mechanism of the mixing process. Later it will be shown that the mixing time is more or less equal to the time required to circulate the liquid once under turbulent conditions. During that time a continuous flow of liquid to be mixed passes the stirrer, giving a striae image of fairly constant intensity. When all the liquid has passed the intensity immediately decreases.

The moment of disappearance of the striae is dependent on the sensitivity of the method. However, by taking as the end point the moment immediately after the sudden decrease in intensity of striae (as indicated in the figure), the influence of the sensitivity is very small. It appears that the reproducibility is better than 5% for various sensitivities of the set-up. The apparatus could detect the striae formation occurring with a difference in refractive index of 10^{-5}, under normal operating conditions. The difference in refractive index between the two starting liquids is of the order of 10^{-2}.

For laminar flow, the end point of mixing is very difficult to determine, as there occurs a gradual transition to the homogeneous state. This is closely connected with the mechanism of the mixing process. In general two effects play a rôle in reaching the uniform state: the long range convective mass transfer effected by the pumping action of the stirrer and the (molecular and eddy) diffusion between the small elements of volume.

In the case of complete turbulence the eddy diffusion is so great that the mixing time is governed by the first effect, i.e. the pumping action of the stirrer. In the case of laminar flow the diffusion is so small that the mixing time is controlled by the diffusion effect.

2.2. Determination of the power consumption

In the course of the present investigation the following methods have been applied for the experimental determination of the power consumption:

a. The stirrer is driven by means of a falling weight connected to the stirrer spindle by a piece of string. After release the weight first falls with an accelerated motion. The rotating stirrer experiences in the liquid a frictional torque which increases with the speed, and hence with the velocity of falling. As soon as this frictional torque has become equal to the torque, exerted by the weight, the motion will be uniform. The distance travelled by the weight per second, multiplied by the weight gives the power consumption of the stirrer. Naturally, the experiment must first be carried out with the stirrer rotating in air, in order to determine the frictional loss in the bearings, so that a correction can be made for this loss.

b. The mixing vessel is placed on a rotary table. If the stirrer axis and the axis of the rotary table are parallel the couple required to prevent rotation of the vessel is equal to the couple exerted by the stirrer (the whole system is at rest and the resultant is therefore equal to zero). The angular velocity multiplied by the couple is equal to the power consumption of the stirrer. This determination must also be corrected for friction in the bearings and is only applied in the case of relatively large torques. For small torques the accuracy is not sufficient.

3. MIXING PERFORMANCE OF THE CONE STIRRER

3.1. The pumping action of the cone stirrer

Observation of the "Schlieren" during the mixing experiment provides useful information on the action of the cone stirrer. Essentially, its effect is that the liquid is displaced downwards. Thus, at the beginning of a mixing experiment the liquid is pumped from the upper layer into the lower layer and there it is, in most cases, intimately mixed with this layer. The liquid-liquid interface will then gradually rise, until eventually it disappears altogether.

It is possible in several cases to measure the rate at which this interface rises and thus to calculate the pumping capacity of the stirrer. From the experimental data a relationship between the mixing time T and the pumping capacity Q can be inferred (fig. 5). This relationship can be represented by the following equation

$$T = k \cdot \frac{V_1}{Q} , \qquad \text{(eq. 1)}$$

where V_1 = the volume of the upper layer.
The dimensionless constant k was equal to 1.4 for a wide range of the variables involved. With very long mixing times deviations occurred, indicated in the graph by a dotted line.

It can be seen from fig. 6 that during the mixing process the pumping capacity is not constant, but decreases slightly. This is due to an increasing counter-pressure which the pumping cone stirrer has to overcome. This counter-pressure is equal to $(\rho_2-\rho_1)gh_1$. For an increase of the interfacial level from h_1 to h_1' the increase in counter-pressure is

$$\Delta P = (\rho_2' - \rho_1)gh_1' - (\rho_2 - \rho_1)gh_1 .$$

If t = the time in which the displaced volume $\int_o^t Q\,dt$ causes the interface to rise to h_1', this expression can, after elimination of ρ_2' and h_1', be elaborated to

$$\Delta P = \frac{(\rho_2 - \rho_1)\int_o^t Q\,dt}{V_2 + \int_o^t Q\,dt} \left(\frac{V_2}{\frac{\pi}{4}(D^2 - d^2)} - h_1 \right)$$ See fig.

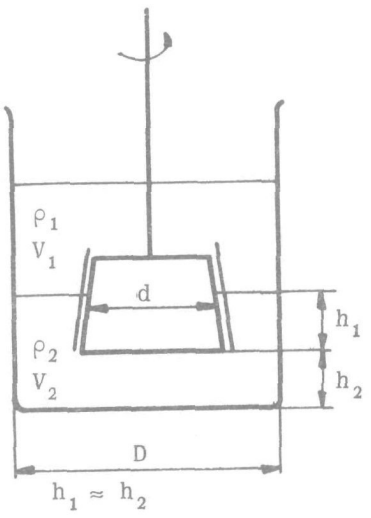

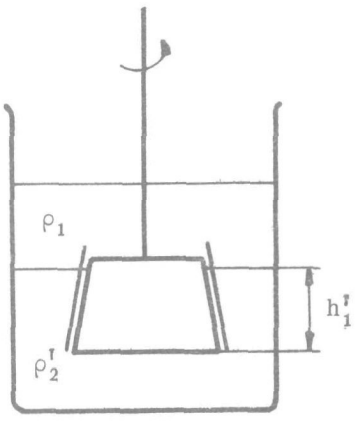

$$\rho_2' = \frac{V_2\rho_2 + \rho_1 \int_o^t Qdt}{V_2 + \int_o^t Qdt}$$

$$\int_o^t Qdt \approx \frac{\pi}{4}(h_1' - h_1)(D^2 - d^2)$$

In the case of the cone stirrer and the 2-litre mixing vessel (fig. 1)

$$\frac{V_2}{\frac{\pi}{4}(D^2 - d^2)} - h_1 \approx h_1 ,$$

and then this equation reduces to

$$\Delta P \approx (\rho_2 - \rho_1) g h_1 \frac{\int_o^t Qdt}{V_2 + \int_o^t Qdt}$$

and the relative increase in counter-pressure becomes:

$$\frac{\Delta P}{(\rho_2 - \rho_1) g h_1} \approx \frac{\int_o^t Qdt}{V_2 + \int_o^t Qdt}$$

If $\int_o^t Qdt >> V_2$ the value of

$$\frac{\Delta P}{(\rho_2 - \rho_1) g h_1} = 1$$

and therefore the counter-pressure has just been doubled. In our experiments this maximum is never reached, because $\int_o^t Qdt \leqq V_2$. For $\int_o^t Qdt = V_2$ the counter-pressure has just become 1.5 times as large. Deviations from this theory occur as soon as the interfacial level rises above the upper side of the cone stirrer.

For the determination of the pumping capacity the tangent is drawn at the point t = 0 (see fig. 6). The slope of this line indicates the pumping capacity at the beginning of the experiment.

Fig. 6 also shows that the ratio between pumping capacities at the beginning and at the end of the mixing experiment is much larger for n = 325 than for n = 430 r.p.m. This is entirely confirmed by the relation between mixing time and difference in density (fig. 8), where it can be seen that for n = 325 r.p.m. the influence of $\Delta\rho$ on the mixing time is much greater than when n = = 430 r.p.m.

3.2. Mixing time

3.2.1. *Experiments*

The influence of the following variables on the mixing time has been studied:

a. *Influence of stirrer speed and of difference in density between the two liquid layers* (fig. 7 and 8)

It can be seen from fig. 8 that the mixing time is, in the first instance, a linear function of the difference in density. If this difference becomes much greater the mixing time increases more than linearly. This progressive increase occurs sooner according as the stirrer speed is lower. Fig. 7 shows that an increase in r.p.m. reduces the mixing time. This effect is pronounced especially at low stirrer speeds and large differences in density. On extrapolation at constant stirrer speed towards a difference in density $\Delta\rho = 0$ the mixing time appears to be about inversely proportional to the stirrer speed.

b. *Influence of the viscosity* (table III)

Small changes in viscosity of the liquid layers (10^{-3} to 10^{-4} N sec/m^2) had no marked effect on the mixing time at a higher stirrer speed. However, above a certain value of the viscosity the mixing time increases strongly with viscosity. This value is lower as the stirrer speed is lower. The mixing then loses its turbulent character and a laminar, comparatively stable flow pattern develops, the rate of mixing being very difficult to measure.

c. *Influence of the slid width* (fig. 9)

Fig. 9 shows that a variation in slit width between 3.5 and 6 mm has little influence on the mixing time. At smaller slit widths the mixing time increases very strongly. This phenomenon also shows up in the pumping capacity, fig. 9, which begins to decrease at slit widths smaller than 3.5 mm. The linear rate of flow, obtained by dividing the pumping capacity by the exit slit

area, shows a maximum at a slit width of about 1.5 mm. With narrower slits the loss of energy owing to friction experienced by the liquid flowing downwards begins to gain in importance. As was to be expected, in the case of these narrow slits an increase in viscosity causes a greater increase in mixing time than with wide slits. For wide slits the pumping capacity is almost independent of the slit width. This indicates that then the capacity is chiefly determined by the layer which rotates along with the inner cone.

d. *Position of the interface and of the stirrer*

With a constant height of the cone stirrer above the bottom and a constant total volume of liquid the volume ratio of the two liquids has been varied (fig. 10).

The position of the cone stirrer has no great influence on the mixing time. The distance between the lower side of the cone stirrer and the bottom of the mixing vessel (the clearance) could not be varied very much. A slight minimum in mixing time occurs when the lower face of the stirrer coincides with the interface.

e. *Influence of dimensions of vessel and stirrer on mixing time*

Experiments in a vessel 0.26 m in diameter, with a liquid volume of 0.014 m^3, shows that the pumping capacity does not depend on the size of the vessel. The mixing times found with this vessel were much greater than those calculated with equation (1). This is due to the fact that the radius of action of the stirrer is more or less limited and hardly extends over the whole volume of this larger vessel. In the "dead space", therefore, non-uniformity may continue to exist for a long time.

Experiments with a cone stirrer whose rotating inner cone is 58 mm long gives results from which it can be inferred that the mixing times are about inversely proportional to the square of the cone length.

3:2.2. *Theory and calculations of the pumping capacity*

We have seen that the mixing effect of the cone stirrer is based largely on its pumping capacity. Calculation of the pumping capacity therefore makes it possible to predict the mixing time theoretically. In the following it is shown to what extent the cone stirrer permits calculations and how the values calculated compare with experimental results.

First we shall consider the pumping action of the cone stirrer (see fig.).

The liquid entering the slit will not instantaneously start rotating as a whole, but will gradually be entrained by the rotating inner cone. The phenomena then occurring are called induc-

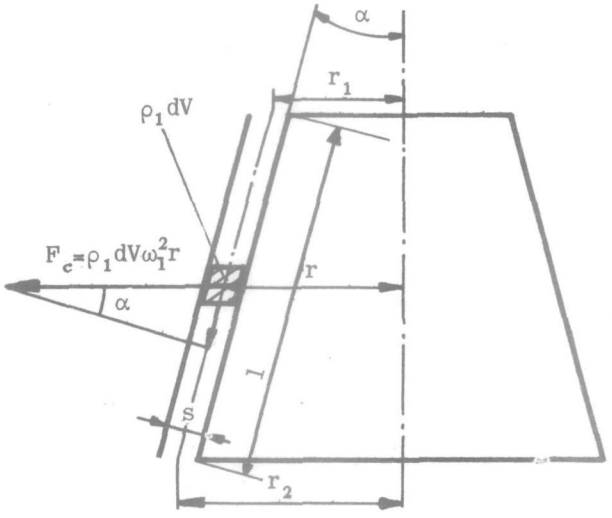

tion phenomena. First the liquid layer nearest to the rotating cylinder wall will be entrained. This moving boundary layer will steadily increase in thickness according as the liquid passes through the slit. Eventually, always provided that the residence time of the liquid in the slit is sufficiently long, a velocity distribution will be reached which remains constant.

We will now compare this induction phenomenon with the flow of a liquid along a flat plate. In this case a boundary layer is formed which gradually increases in thickness in the direction of flow. At the beginning of the plate the boundary layer is laminar, but when it has reached a certain critical value it changes over into a turbulent boundary layer, which in itself consists of a laminar sub-layer and a fully developed turbulent layer.

The velocity distribution in the laminar boundary layer can be calculated from the hydrodynamic equation of motion and from the equation of continuity. BLASIUS has found an exact solution (11), but it does not allow of easy calculations.

A simpler, if not quite exact, solution has been suggested by TAYLOR. He found that the velocity U of the liquid parallel to the plate, at a distance y from the plate, can be approximated by

$$\frac{U}{U_o} = 2\frac{y}{\delta} - \frac{y^2}{\delta^2}$$

where: δ = the thickness of the boundary layer
U_o = velocity of the main liquid stream.

The thickness of the boundary layer at a point x' is:

$$\frac{\delta_{x'}}{x'} = 5.5 \sqrt{\frac{\nu}{U_o x'}}$$

where x' = distance in direction of flow from the leading edge of plate

ν = kinematic viscosity of liquid.

The laminar boundary layer passes into a turbulent boundary layer when

$$Re_\delta = \frac{U_o \delta}{\nu} \geqq 1200 \qquad \text{or} \qquad Re_{x'} = \frac{U_o x'}{\nu} \geqq 5.10^4$$

The velocity distribution in a turbulent boundary layer cannot entirely be determined by theoretical calculations. It is, however, possible, with reference to the theory of turbulence, to calculate the general shape of the curve; for the rest, it has to be adapted to the experiments. This velocity distribution is known as the logarithmic velocity distribution (11).

In practice, the velocity distribution can also be closely approximated by a simple 1/7-power function:

$$\frac{U}{U_o} = \left(\frac{y}{\delta}\right)^{1/7}$$

The thickness of the boundary layer is then given by

$$\frac{\delta}{x'} = 0.371 \left(\frac{\nu}{U_o x'}\right)^{1/5}$$

These relations also apply to the case of a moving plate and a stationary liquid. In that case U_o is the velocity of the moving plate.

The rotating inner cone can now be considered as the moving plate and the length x' parallel to the plate is then the length of the screw-path travelled by the liquid particle after entering the slit.

For the present it will be assumed that the velocity distribution of the liquid in the slit is approximated by the above-mentioned equations.

Let us first calculate the work done on a unit mass of liquid in the case of a turbulent boundary layer.

Consider an annular element of volume $2\pi r dx dy$

x = co-ordinate in direction of slit

y = distance normal to inner cone.

The work per unit mass then becomes

$$W = \frac{\int_t \int_x \int_y v_x \, (\sin \alpha) \, \omega_1^2 \, r \, 2\pi r dx dy dt}{\int_x \int_y 2\pi r dx dy}$$

ω_1 = angular velocity of liquid.

Now $$\omega_1 = \omega \left\{ 1 - \left(\frac{y}{\delta}\right)^{1/7} \right\}$$

and $$W = \frac{\int_t \int_x \int_y v_x \sin \alpha r \omega^2 \left\{ 1 - \left(\frac{y}{\delta}\right)^{1/7} \right\}^2 2\pi r dx dy dt}{\int_x \int_y 2\pi r dx dy}$$

In the integration over y, v_x is assumed to be constant. The integration must be performed between the limits y = 0 and y = δ. This produces:

$$W = \frac{\int_t \int_x \frac{1}{36} \delta \, v_x \sin \alpha r \omega^2 \, 2\pi r dx dt}{\int_x \int_y 2\pi r dx dy}$$

Now

$$\delta = 0.371 \; x'^{4/5} \; \nu^{1/5} (\omega r)^{-1/5} \; .$$

The length x' is practically equal to $x' = \omega r \frac{x}{v_x}$ (for $\omega r >> v_x$). Thus

$$W = \frac{\int_t \int_x \frac{1}{36} \cdot 0.371 \left(\frac{x}{v_x}\right)^{4/5} \nu^{1/5} (\omega r)^{3/5} \, v_x \, (\sin \alpha) \, r\omega^2 \, 2\pi r dx dt}{\int_x \int_y 2\pi r dx dy}$$

$$W = \frac{\int_t \frac{1}{36} \cdot 0.371 \cdot 5/9 \; l^{9/5} \; \nu^{1/5} \; (\omega r)^{8/5} \; v_x^{1/5} \; (\sin\alpha) \omega \, 2\pi r dt}{\int_x \int_y 2\pi r dx dy}$$

The integration over t has to be performed between the limits t = 0 and t = residence time in the slit. This residence time is

$$\frac{I}{2\pi r s v_x} \, , \quad \text{where I = volume of slit:} \quad I = \int_x \int_y 2\pi r dx dy.$$

Thus,

$$W = \frac{1}{36} \cdot 0.371 \cdot 5/9 \; l^{9/5} \; \nu^{1/5} \; (\omega r)^{8/5} \; v_x^{-4/5} \; (\sin \alpha) \; \omega \, s^{-1}$$

$$W = 0.68 \; \nu^{1/5} \; v_x^{-4/5} \; l^{9/5} \; n^{13/5} \; r^{8/5} \; (\sin \alpha) \; s^{-1} \; .$$

In the integration over x the radius r and the velocity v_x are

kept constant, for r the average $r = \frac{r_1 + r_2}{2}$ is taken and for v_x the corresponding velocity is filled in. The error thus made is negligible. The expression for W when using r_2 and v_{xr_2} is

$$W = 0.49\ \nu^{1/5}\ v_{xr_2}^{-4/5}\ l^{9/5}\ n^{13/5}\ r_2^{8/5}\ (\sin\alpha)\ s^{-1} \quad \text{(eq. 2a)}$$

In deriving this equation it was assumed that the thickness of the boundary layer and the velocity distribution in the boundary layer is not affected by the presence of the solid stator wall. Actually this is not true. Moreover, in the case under consideration the flow pattern is not so simple as for a flat plate, but becomes more intricate owing to secondary vortices. These arise because the rapidly rotating liquid near the wall is whirled outward by the centrifugal force, which results in an increase in angular momentum transfer in the radial direction (y). When the turbulent boundary layer has thickened to such an extent that the stator wall is reached, another boundary layer will built up on that wall, until a state of equilibrium is reached, the angular momentum $\omega_1 r^2$ being constant for a large part (about 80%) of the slit width.

Measurements carried out by TAYLOR have shown that $\omega_1 \approx 0.45\omega$ rotor (36, 37, 38). Near the walls the boundary layer condition with its large velocity gradient persists. This stationary condition will practically have been reached when the boundary layer that would form if no stator wall were present is very thick as compared with the slit width. In our experiments this hypothetical thickness is of the order of magnitude of 10 mm. Thus, when leaving the slit, this boundary layer has grown to a few times the slit width, but it must not yet be supposed that the stationary condition has been completely reached.

As a result of the centrifugal force F_c the liquid will be forced downwards, the kinetic energy thus imparted to the liquid emerging from the slit is equal to $\frac{1}{2} v_x^2$ per unit mass. Besides, the liquid issuing from the slit will have a potential energy, due to the fact that the liquid of density ρ_1 enters a liquid of density ρ_2. When the interface between the two liquids has reached a height h above the underface of the stirrer, the potential energy per unit mass is

$$\frac{\rho_2 - \rho_1}{\rho_1}\ gh = \frac{\Delta\rho gh}{\rho_1}$$

We now assume that the work done by the cone stirrer serves entirely to impart kinetic and potential energy to the liquid and to overcome the loss L due to friction experienced by the liquid emerging from the slit. Then we have

$$W = \tfrac{1}{2} v_{xr_2}^2 + \frac{\Delta \rho g h}{\rho_1} + L \qquad \text{(eq. 2b)}$$

In principle it is possible to calculate from this equation v_{xr_2}, the pumping capacity Q ($Q = 2 \pi r_2 s v_{xr_2}$) and the mixing time $T = \frac{1.4\, V_1}{Q}$.

Frictional loss in the slit

For calculation of the frictional loss L of the liquid flowing through the slit in the axial direction use can be made of the well-known equations for the flow in ducts.

The diameter is the so-called hydraulic diameter, which in the case of the cone stirrer is equal to twice the slit width. Ignoring for the present the influence of rotation, we have, for

$$Re = \frac{\rho v_x . 2s}{\mu} < 2000$$

$$\Delta p = 12\mu \frac{v_x}{s^2} l = \frac{l}{2s} \frac{96}{Re} . \tfrac{1}{2} \rho v_x^2 \qquad \text{(if } s \ll r\text{)}.$$

For Re > 2000 we have

$$\Delta p = \frac{0.316}{Re^{0.25}} . \frac{l}{2s} \tfrac{1}{2} \rho v_x^2 .$$

Our measurements have been made at values of Re of the order of 2000. At Re = 2000 both equations give the same answer, which, at a slit width s = 6.5 mm, gives a pressure drop of

$$\Delta p = 0.15 . \tfrac{1}{2} \rho v_x^2 \ (= 15\% \text{ of the kinetic energy}).$$

This shows that in most cases the pressure loss may be neglected.

Measurements by TAYLOR, FAGE and CORNISH (8,35) showed that owing to the rotation of the inner cone (or cylinder) above a certain critical speed n_c, the pressure loss in somewhat higher than for a non-rotating inner cone (cylinder). This critical speed n_c is given by

$$\frac{2 \pi n_c r s}{\nu . 60} \sqrt{\frac{s}{2(2r+s)}} = 22$$

Moreover, n_c increases somewhat with the rate of flow in axial direction. For the conventional slit width s = 6.5 mm, n_c = 240 r.p.m. For $n > n_c$ the pressure loss will therefore be somewhat greater than the above equations show. For the calculations of the pumping capacity these corrections, however, are insignifi-

cant. The influence of the velocity distribution of v_x over the slit width both on the pressure loss and on the other terms in the equation of energy will also be neglected.

In a similar way expressions for W can be derived for a laminar boundary layer and in the case where there is a linear change in angular velocity of the liquid between the two cones in the whole slit (Couette flow). The laminar boundary layer occurs at the entrance of the slit (the beginning of the plate) and must be taken into account when using very small and short cones. The Couette flow occurs in the case of very narrow slits, if there is a uniform velocity distribution in the slit. Schematically the calculations can be summed up as follows:

Induction range	*Condition*
$W = 24\, \nu^{½} \sin\alpha\, n^2\, r_2\, l^{3/2}\, s^{-1}\, v_{xr_2}^{-½}$	$\frac{(\omega r)^2 x}{\nu\, v_x} < 5.10^4$ (laminar boundary layer)
$W = 0.49\, \nu^{1/5} \sin\alpha\, n^{13/5}\, r_2^{8/5}\, l^{9/5}\, s^{-1}\, v_{xr_2}^{-4/5}$ (eq. 2a)	$\frac{(\omega r)^2 x}{\nu\, v_x} > 5.10^4$ (turbulent boundary layer)
Stationary condition	$(\frac{\omega r s}{\nu})^2 \frac{s}{r} \leqq 2710$ and *)
$W = \frac{\omega^2}{6\pi} \sin\alpha \frac{I}{w}$	$\delta = 0.37\, (\frac{x}{v_x})^{4/5}\, \nu^{1/5}\, (\omega r)^{3/5} >> s$ Couette flow

*) S. Goldstein (11) Modern developments in fluid dynamics p. 389.

3.2.3. *Comparison of theory with the experimental mixing times*

Since most of the experiments satisfy the conditions

$$\frac{(\omega r)^2 x}{v_x \nu} > 5.10^4 ,$$

equation (2a) was used to determine the pumping capacity for some cases. By means of equation (1) the mixing time can be calculated from the pumping capacity. The calculations were based on the assumption that

$$W = 0.49\ \nu^{1/5}(\sin\alpha)\ n^{13/5} r_2^{8/5} l^{9/5} s^{-1} v_{xr_2}^{-4/5} = \tfrac{1}{2}\, v_{xr_2}^{2} + \frac{\Delta\rho g h}{\rho_1} \qquad \text{(eq. 2c)}$$

In figs. 7, 8 and 9 the pumping capacities and mixing times calculated from the above-mentioned equation have been plotted (dotted line), the experimental curves being given for comparison.

The increase in velocity for smaller slit widths is perfectly clear (fig. 9). For slits $s < 1$ mm the frictional resistance becomes important and the velocity begins to decrease again.

The changes in mixing time with the density (fig. 8) are also represented fairly accurately by the theoretical curve, just like the relation between mixing time and stirrer speed (fig. 7). It may be remarked that for a large T,

$$T > \frac{1.4\ V_1}{Q}$$

(fig. 5), so that the theoretical mixing time calculated from equation (1) will then become too small.

3.3. Power consumption

3.3.1. *Experiments*

Influence of the stirrer speed

Fig. 11 shows that the power consumption P gives a straight line if plotted against the stirrer speed n on a double logarithmic scale. This relationship may be formulated as follows:

$$P \sim n^{(2.7 \text{ to } 2.8)}\ .$$

Variation of the slit width has no appreciable effect on the power consumption.

Viscosity

If the relationship between power consumption P and viscosity μ is written as

$$P \sim \mu^{a}\ ,$$

it has been found that the exponent, a, is about 0.35 at low viscosities and high stirrer speeds and is about equal to unity at high viscosities and low stirrer speeds (laminar flow).

Fig. 12 gives, in the way usually found in the literature on stirring, the relation between the dimensionless power factor $\left(\frac{P}{\rho n^3 d^5}\right)$ and Reynolds' number $\left(\frac{\rho n d^2}{\mu}\right)$. The gradual transition from laminar to turbulent flow occurs at Re ≈ 300.

3.3.2. *Calculations*

We shall now calculate the power consumption for the case of a turbulent boundary layer in the slit. The power consumption

$$P = \omega M = 2\pi n \; 2\pi r^2 \int_o^1 \tau_\omega dx ,$$

M = the torque exerted by the stirrer.

From the equation of momentum the following expression for the wall shearing stress follows (11):

$$\tau_\omega = -\rho \frac{d}{dx'} \int_o^\delta (U^2 - UU_o) dy$$

If for U we take $U = U_o \left(\frac{y}{\delta}\right)^{1/7}$ this becomes

$$\tau_\omega = -\rho \, U_o^2 \, . \, 7/72 \, \frac{d\delta}{dx'} .$$

Now $\delta = 0.371 \; x'^{4/5} \left(\frac{\nu}{U_o}\right)^{1/5}$, therefore

$$\tau_\omega = 7/72 \, . \, 4/5 \, . \, 0.371 \left(\frac{\nu}{U_o x'}\right)^{1/5} \rho U_o^2 =$$

$$= 0.029 \left(\frac{\nu v_x}{x}\right)^{1/5} \rho (\omega r)^{8/5}$$

if $$x' = (\omega r) \frac{x}{v_x} .$$

This value for τ_ω substituted in the formula for P gives

$$P = 27.5 \; \rho n^{13/5} \; r^{18/5} \; \nu^{1/5} \; v_x^{1/5} \; l^{4/5} \qquad \text{(eq. 3)}$$

When for r and v_x average values are substituted eq. 3 gives a theoretical value for power consumption, which has been plotted in fig. 11 as a function of the speed of rotation.

As the power consumption was mostly measured in water we substituted in eq. 3 for v_x the linear velocity at $\Delta\rho = 0$.

3.3.3. *Comparison with the experimental curve*

This shows very satisfactory agreement between calculation and experiment (fig. 11).

If the power consumption as expressed in eq. (3) is compared with the power consumption due to the pumping capacity of the cone stirrer, as can be derived from equation (2a), we find for this ratio:

$$\frac{P \text{ eq. } (3)}{P \text{ eq. } (2a)} = 37, \quad \text{where } P \text{ eq. } (2a) = W.2\pi rsv_x .$$

Hence, the power consumption, necessary for the pumping action is only 2.7% of the total power consumption of the stirrer, the rest is consumed for the generation of the rotational movement of the liquid between the two cones.

3.4. Mixing energy

Multiplication of the measured mixing time by the corresponding power consumption of the stirrer yields the energy consumed for complete mixing. Fig. 13 shows that there is a stirrer speed at which this mixing energy reaches its minimum. This speed is higher according as the difference in density between the two liquid layers is greater.

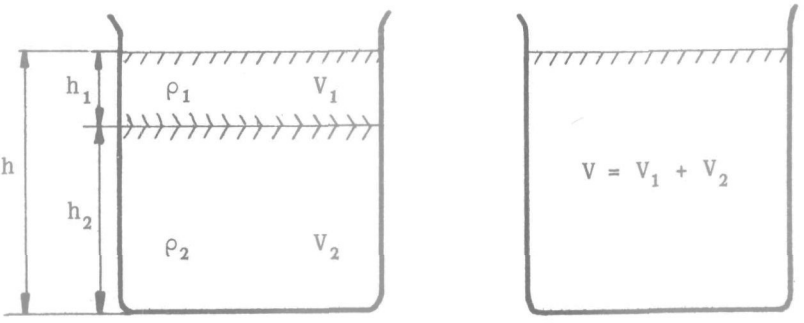

Situation 1 Situation 2

The potential energy content of the liquid after mixing is greater than before mixing.

The theoretical minimum of mixing energy required can be calculated as follows (see fig.). In situation 1 the potential energy with respect to the bottom of the vessel of the two liquid layers is

$$E_{pot_1} = V_1\rho_1 g\,(h_2 + \tfrac{1}{2}h_1) + V_2\rho_2 g\,(\tfrac{1}{2}h_2) .$$

In sutuation 2 the potential energy is equal to

$$E_{pot_2} = (V_1 + V_2)\left(\frac{\rho_1 V_1 + \rho_2 V_2}{V_1 + V_2}\right) g \cdot \tfrac{1}{2}(h_1 + h_2).$$

The increase in potential energy becomes:

$$E = E_{pot_2} - E_{pot_1} = \tfrac{1}{2} V_1 h_2 (\rho_2 - \rho_1) g$$

if $\frac{V_1}{V} = \varphi$ $\qquad E = \tfrac{1}{2} \varphi (1 - \varphi)\, Vh\, (\rho_2 - \rho_1) g$.

The increase E represents the theoretical minimum of mixing energy required. It can reach a maximum of 0.125 $Vh(\rho_2 - \rho_1)g$. In that case $\varphi = \tfrac{1}{2}$, i.e. the two liquid volumes V_1 and V_2 are equal to each other. In our experiments this is the normal case. The theoretical mixing energy then becomes 0.015 $g(\rho_2 - \rho_1)$ Nm/m^3 (h = 120 mm). On comparing this energy with the energy found at optimum speed, as shown in fig. 13, we find that the theoretical mixing energy is only about 1.5% of the mixing energy actually required (in the case of $\Delta\rho = 74$ kg/m^3). The remaining 98.5% is converted as kinetic energy into heat of friction. Comparing this 1.5% with the 2.7% of the pumping action (see 3.3.3) it can be seen that in this case about half of the pumping energy is converted into potential energy.

4. MIXING PERFORMANCE OF PADDLE STIRRERS, PROPELLER STIRRERS AND TURBOMIXERS

4.1. Mixing time

4.1.1. *Dimensional considerations*

In the same way as with the cone stirrer, the mixing time was determined as a function of a number of variables.

The mixing time T is found to depend on the following liquid properties:

μ = final viscosity of the mixed product
ρ = density of mixed product
$\Delta\rho$ = difference in density between the liquids to be mixed

and on the stirring conditions:

n = number of revolutions of stirrer in unit time
d = diameter of stirrer
D = diameter of vessel
H = height of liquid in vessel

Moreover it must depend on g, acceleration of gravity.

Other factors which influence the mixing are the location and the mounting of the stirrer (eccentricity), the ratio by volume of the liquids to be mixed, the shape of the vessel (presence of baffles) and the shape of the stirrer.

Let us first consider the mixing time T as a function of (n, μ, ρ, $\Delta\rho$, d, D, H, g). Together with T these quantities can be combined to 9-3 = 6 dimensionless groups. For these groups we have taken:

1) $\frac{Tnd^3}{V}$, where V = volume of the liquid ($V \sim D^2H$)

2) $\frac{\rho nd^2}{\mu}$ = Reynolds' number

3) $\frac{n^2d^2}{gH}$ = Froude number

4) $\frac{\rho}{\Delta\rho}$

5) $\frac{d}{D}$

6) $\frac{H}{D}$

The above quantities have been adapted to the mechanism of mixing, so that they also have a physical significance. As has

already been said, the mixing time is mainly determined by the pumping capacity Q of the stirrer. Accordingly, mixing time is proportional to the time required to pump all the liquid around once: $T \sim \frac{V}{Q}$. Thus $\tau = \frac{TQ}{V}$ represents the number of times that the volume of liquid has to be pumped around. Dimensionally the expression for the pumping capacity has the form $Q = nd^3$. However, it is obvious that in correlations expressions for the theoretical pumping capacity have to be used which take into account not only the diameter d of the stirrer, but also the type, the shape and other dimensions of the stirrer (see table, Pumping Capacity 4.2.4). The dimensionless mixing time τ is then given by $\frac{TQ_{th}}{V}$.

In these expressions for the pumping capacity only stirrer dimensions are involved. During mixing, however, also other factors affect the actual pumping capacity. The rotating stirrer, for instance, has to overcome a certain counterpressure, because liquid of lower density has to be pushed into liquid of higher density, thus reducing the pumping capacity of the stirrer. This influence is characterized by a density Froude number giving the ratio between the dynamic head of the flowing liquid, which is assumed to be proportional to $\rho n^2 d^2$, and the static head $\Delta\rho gH$ that has to be overcome. This quantity corresponds to the product of the dimensionless groups mentioned in 3 and 4. With decreasing values for the quantity $\frac{\rho n^2 d^2}{\Delta\rho gH}$ the mixing time will naturally increase.

The dimensionless mixing time τ will also depend on the condition of flow in the mixing vessel, i.e. on Reynolds' number $\frac{\rho nd^2}{\mu}$ $(= \frac{nd^2}{\nu})$.

Finally, various length ratios play a rôle, notably those which give the dimensions of the stirrer in comparison with the total liquid volume. If the vessel is too large or of unsuitable dimensions in relation to the dimensions of the stirrer, "dead corners" with little turbulence will be formed, which lengthen the mixing time.

The expression for the mixing time may now be formulated as $\tau = f\left(\frac{nd^2}{\nu}, \frac{\rho n^2 d^2}{\Delta\rho gH}, \frac{d}{D}, \frac{H}{D}\right)$.

During the correlation of the data we tried to represent the right-hand term by a product of functions, viz.

$$\tau = f_1\left(\frac{nd^2}{\nu}\right) f_2\left(\frac{\rho n^2 d^2}{\Delta\rho gH}\right) f_3\left(\frac{d^3}{D^{2.5}H^{0.5}}\right) \qquad (4)$$

It is obvious that this will not always be possible. However,

here good results were obtained with the above-mentioned procedure.

4.1.2. *Influence of the density Froude number* $\frac{\rho n^2 d^2}{\Delta\rho g H}$ *on* τ

This relation is given for the various types of stirrer in figures 14, 15, 16 and 17.

The measurements on which the graphs are based were carried out in a region where Reynolds' number and the length ratios have little influence. In a large region the relation may be represented by a power function:

$$\tau \sim \left(\frac{\rho n^2 d^2}{\Delta\rho g H}\right)^{+a} \tag{5}$$

where for a paddle stirrer $a = -0.3$
a paddle stirrer with inclined blades $a = -0.35$
a turbomixer $a = -0.3$
a propeller stirrer $a = -0.25$

For $\Delta\rho = 0$ the mixing time T approaches a finite positive value, which may be determined by extrapolation to $\Delta\rho = 0$ in a T vs $\Delta\rho$ graph; hence for very high $\frac{\rho n^2 d^2}{\Delta\rho g H}$ values τ approaches a limiting value.

We have also applied an injection method in some cases. Mixing-time measurements were carried out by suddenly adding a small amount of a glycerine-water mixture to the water during stirring, and measuring the time necessary for the striae to disappear. The results are indicated in the figures 14, 15, 16, 17. The values found are invariably higher than the limiting values found by extrapolation to $\Delta\rho = 0$ in a T vs $\Delta\rho$ graph, which suggests that in our experiments the quantity $\frac{\rho n^2 d^2}{\Delta\rho g H}$ still has some influence.

In addition to these experiments the influence of the volume ratio between the two liquids to be mixed was investigated (table XIII). The results resemble those found with the cone stirrer (fig. 10). As we saw in 3.4, the increase in potential energy for a volume ratio of $\frac{\varphi}{1-\varphi}$ between the two liquids to be mixed, at a constant total liquid volume, is equal to $\frac{1}{2}\varphi(1-\varphi)\,\Delta\rho g H$. If now for the density Froude number we take $\frac{\rho n^2 d^2}{4\,\varphi(1-\varphi)\,\Delta\rho g H}$, instead of $\frac{\rho n^2 d^2}{\Delta\rho g H}$ (which are equal for the normal case of $\varphi = 0.5$), the results of the experiments with a varying φ can be correlated in the normal graph of dimensionless mixing time versus density Froude number.

4.1.3. *The influence of Reynolds' number* $\frac{\rho n d^2}{\mu}$

This relation is given in figures 18 and 19. For values $Re > 10^3$ to 10^4 the quantity $\tau . \left(\frac{\rho n^2 d^2}{\Delta \rho g H}\right)^{-a}$ proved to be nearly constant.

For lower values it increases rapidly ($\tau . Fr^{0.3} \sim Re^{-3}$). The type of flow is laminar, with persistent liquid eddies that show little exchange with their surroundings. Inhomogeneities are particularly persistent in the "dead corners".

The behaviour of the streamlines also revealed, for all stirrers studied, a transition from the laminar to the turbulent state. The streamlines could be made visible by introducing little gas bubbles into the rotating liquid. At a certain critical stirrer speed the track of the gas bubbles becomes irregular. The change gradually set in at a value of the Reynolds' number: $Re_{transition} \simeq 250$.

In the laminar region the mixing mechanism is no longer controlled by the pumping capacity but by the exchange between the more or less persistent liquid eddies. The concentration at a given point in the vessel approaches the equilibrium concentration much more gradually and there is no question of a sharp transition from not-yet-uniform to uniform composition of the liquid, as in the case in the turbulent range. In the laminar region accurate measurement of the mixing time from the striae image is not possible.

4.1.4. *Influence of dimensions of vessel relative to stirrer dimensions*

The relation is shown in fig. 20. It was possible to include the $\frac{d}{D}$ and the $\frac{H}{D}$ ratio in one combination viz. $\frac{d^3}{D^{2.5} H^{0.5}}$. This quantity may also be written as $\left(\frac{H}{D}\right)^{0.5} . \frac{d^2}{V}$ and more or less represents the ratio between stirrer volume and vessel volume.

In the range $10^{-3} < \frac{d^3}{D^{2.5} H^{0.5}} < 4 \times 10^{-2}$ the quantity $\tau . \left(\frac{\rho n^2 d^2}{\Delta \rho g H}\right)^{-a}$ is practically constant; outside this range it increases. For $\frac{d^3}{D^{2.5} H^{0.5}} < 10^{-3}$ the vessel volume is so large that dead corners are formed which lengthen the mixing time, whereas for $\frac{d^3}{D^{2.5} H^{0.5}} > 4 \times 10^{-2}$ the vessel volume is so small, relative to the stirrer volume, that the movement of the liquid by the stirrer is impeded by the proximity of the vessel wall. For $\frac{d^3}{D^{2.5} H^{0.5}} > 10^{-1}$ the relation can be represented by a power function:

$$\tau \left(\frac{\rho n^2 d^2}{\Delta \rho g H}\right)^{-a} \sim \left(\frac{d^3}{D^{2.5} H^{0.5}}\right)^{+1}$$

4.1.5. *Influence of the location of the stirrer, etc.*

Eccentricity of the stirrer

From the curves shown in figures 14-20 dealt with above it is apparent that the behaviour of all types of stirrers is about the same. However, differences in the behaviour of stirrers occur when they are positioned eccentrically.

By eccentricity we understand the distance between the stirrer shaft and the axis of the mixing vessel divided by half the diameter of the vessel. The influence of eccentricity on mixing time is shown in fig. 21. Unlike the influences discussed above, this influence proves to be greatly dependent on the type of stirrer. In the case of stirrers causing axial flow, like the propeller stirrer and the paddle stirrer with inclined blades, eccentricity shortens the mixing time. This is due to an increase in the relative velocity of the rotating stirrer and the liquid rotating with it. With an eccentric stirrer this relative velocity will be greater than when it is centrally placed. As will appear in 4.2.3 greater relative velocity causes a greater axial pumping capacity and therefore a shorter mixing time. In the case of stirrers causing tangential and radial flow, like the paddle stirrer (with straight blades) and the turbomixer, eccentricity lengthens mixing time. Tangential and radial pumping capacity also increase as the relative velocity increases. As, however, here the vicinity of the wall impedes the flow of liquid in a radial direction, mixing time becomes longer.

In the case of a paddle stirrer with the blades set at an angle α of 40° to 50°, mixing time is found to be independent of eccentricity, so it may be assumed that here the two effects counterbalance each other.

Influence of the clearance between stirrer and bottom of the vessel

For a propeller stirrer this influence has been investigated by KRAMERS and KNOLL (21). Their measurements show that a clearance equal to half the liquid height generally ensures the shortest mixing time. Our own experiments with a paddle stirrer pointed in the same direction (fig. 22). The investigation into the influence of this variable was therefore discontinued. Unless otherwise stated the clearance was therefore in all experiments equal to half the liquid height.

Influence of inclination of the stirrer haft

Rotation of the liquid with the stirrer can be suppressed not only by eccentric position of the stirrer, but also by setting the stirrer in an inclined position in the mixing vessel. When the stirrer shaft of a propeller is set at an angle of 30^{o} or more to the axis of the mixing vessel, mixing time becomes about 0.7 times the mixing time under normal conditions. This effect is therefore of the same magnitude as the influence of eccentricity of the stirrer.

Influence of baffles

In the experiments with baffles, only the assembly as indicated in fig. 2A has been investigated. This type of baffles (mounted at right angles to the wall of the vessel) is commonly used in practice.

The object of baffles in the mixing vessel is to prevent the liquid from rotating with the stirrer. The ensuing advantage is that this counteracts vortex formation, which beats air into the liquid. Moreover, baffles cause the flow of liquid to be directed more axially, which generally has a favourable effect on the rate of mixing. In the case of propeller stirrers baffling has the same effect on mixing time as eccentricity of the stirrer, expecially at higher rotor speeds. The relative velocity of the stirrer and the liquid then approaches the stirrer speed, resulting in a higher pumping capacity. At lower rotor speeds baffling has less influence on the flow pattern and on the mixing time.

With paddle stirrers and turbomixers baffling has about the same influence on mixing time as with propeller stirrers. Turbomixers are often provided with deflecting stator blades, resulting in a perfectly radial flow pattern.

4.2. **Pumping capacity** (Influence of shape and dimensions of stirrer)

4.2.1. *Paddle stirrers and turbomixers*

When calculating the dimensionless mixing time $\tau = \frac{TQth}{V}$, the theoretical pumping capacity Qth must be expressed in characteristic, measurable quantities of the stirrer.

We shall deal successively with the pumping capacities of the paddle stirrers (with straight blades), the turbomixer, the paddle stirrer with inclined blades and the propeller stirrer.

The paddle stirrer with blades set at right angles imparts to the liquid a momentum that gives it a tangentially rotating movement. From the point of view of mixing this movement is undesir-

able, because it does not contribute to mixing in a vertical direction and so cannot counteract the influence of gravity. That the paddle stirrer nevertheless has a good mixing effect is because a secondary radial flow pattern is formed due to the centrifugal forces set up.

The flow pattern of the turbomixer greatly resembles that of the paddle stirrer. Here too a radial flow is set up by centrifugal forces. Only the pumping capacity due to this radial flow has been considered. Since the shape and action of the turbomixer is identical to that of the centrifugal pump, the expression for the pumping capacity of a centrifugal pump can be used.

From the theory of centrifugal pumps it follows that the theoretical energy per unit volume leaving the centrifugal pump (known as "Euler's head") is equal to $h_E = \frac{c_2\ \omega r_2\ \cos a_2}{g}$, where

c_2 = absolute discharge velocity of the liquid from the vane.
α_2 = the angle that c_2 forms with the tangent to the circle having a radius r_2,
r_2 = radius of vane wheel (see figure).
β = vane angle
ω = angular velocity

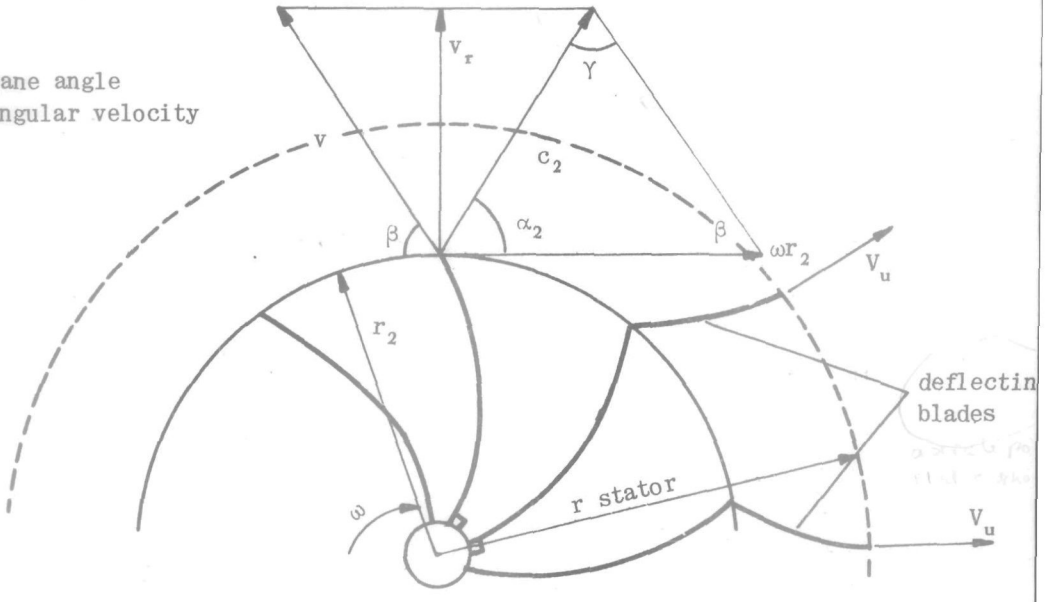

Discharge velocity diagram of turbomixer

According to Bernoulli's law: $h_E = h_{kin} + h_{stat}$ if friction losses in the pump are neglected.

In the case where no deflecting blades are present $h_{kin} = \frac{1}{2} c_2^2/g$. The static head h_{stat} is assumed to be equal to the

head $\frac{1}{2}(\omega\ r_2)^2/g$, if ω_1 = the angular velocity of the rotating liquid in the vessel.

So

$$\rho c_2\ \omega r_2\ \cos\alpha_2 = \frac{1}{2}\rho c_2^2 + \frac{1}{2}\rho(\omega_1\ r_2)^2$$

If $\frac{\omega_1}{\omega} = q (q < 1)$, then it follows that $v_{rad} = c_2 \sin\alpha_2 = \omega r_2 \sin\beta \sqrt{1-q^2}$, where β stands for the vane angle between the blades and the tangent to the circle having a radius r_2.

In the case that $q = 0$, $\alpha_2 = \gamma$ and $c_2 \sin\alpha_2 = \omega r_2 \sin\beta$.

The radial pumping capacity is the product of the annular area $2\pi r_2 w$ and v_{rad}; therefore radial pumping capacity $Q = 4\pi^2 n r_2^2 w \sin\beta\sqrt{1-q^2} = \pi^2 n d^2 w \sin\beta\sqrt{1-q^2}$. In the case of a paddle stirrer $\beta = 90^\circ$ and $\sin\beta = 1$, therefore $Q = \pi^2 n d^2 w\sqrt{1-q^2}$.

If all the liquid in the vessel is rotating with an angular velocity ω, then $q = 1$ and $Q = 0$.

If baffles are present $q = 0$ and $Q = \pi^2 d^2$ wn $\sin\beta$. The dimensionless mixing time $\tau = \frac{TQth}{V}$ becomes $\tau = \frac{Tnd^2 w\ \pi^2\ \sin\beta}{V}$ and in the case of paddle stirrers $\tau = \frac{Tnd^2 w\ \pi^2}{V}$.

When deflecting blades are present (as is often the case with turbomixers), again $h_E = h_{kin} + h_{stat}$. If v_u is the discharge velocity of the liquid from the stator, $h_{kin} = \frac{1}{2}\rho v_u^2$. If no rotation of the liquid in the vessel occurs h_{stat} may be assumed to be zero, hence $\rho c_2 \omega r_2 \cos\alpha_2 = \frac{1}{2}\rho v_u^2$. Now $v_u = k c_2 \sin\alpha$, if $k = \frac{r_2}{r_{stator}}$. The radial velocity $c_2 \sin\alpha$ now becomes

$$c_2 \sin\alpha \quad \frac{\omega r_2(-1 + \sqrt{1 + 2k^2\ tg^2\ \beta})}{k^2\ tg\ \beta}.$$

In many constructions $k \approx 0.7$, so $k^2 \approx \frac{1}{2}$, which gives:

$$c_2 \sin\alpha \approx 2\ \omega r_2 \left(\frac{1 - \cos\beta}{\sin\beta}\right).$$

Compared with the turbomixers without deflecting blades, the pumping capacity is now by a factor $\frac{2}{1 + \cos\beta}$ larger. Theoretically, the pumping capacity would become infinitely large for $\beta = 180^\circ$. In practice the velocities become for $\beta > 90^\circ$ so high that friction losses become important. As $\frac{1}{2}\rho c_2^2 + (h_{stat})_{rotor} = \frac{1}{2}\rho v_u^2 + 0$ and $c_2 > v_u$, $(h_{stat})_{rotor} < 0$, which means that liquid will flow into the slit between rotor and stator. As a consequence $(h_{stat})_{rotor}$ will increase, and v_u, and hence the pumping capacity will decrease.

A gradual transition from paddle stirrer to turbomixer (with-

out deflecting blades) could be studied by curving the blades and investigating the influence of β.

From experiments in which the influence of the vane angle β of a two-bladed stirrer on mixing time was determined (the vane blade being curved in an arc), it was found that the inclusion of a factor sin β in the formula for dimensionless mixing time also has experimental significance (fig. 23). The linear relation between sin β and $\frac{1}{T}$ suggests linearity between sin β and Q. Extrapolation to sin $\beta = 0$ produces a finite value for T, though then the theoretical radial pumping capacity would have to become zero. Apparently there is still some flow which causes mixing.

The influence of the blade width w on τ was experimentally determined. It is evident from table IX that Q is proportional to w for values of $\frac{w}{d}$ less than 0.5, which is in agreement with the above-mentioned expression $\tau = \frac{Td^2wn\ \pi^2}{V}$. For $\frac{w}{d}$ values of more than 0.5 τ increases with increasing $\frac{w}{d}$, i.e. Q is then less than proportional to w.

4.2.2. *Paddle stirrer with inclined blades*

A form of stirrer intermediate between the paddle stirrer and the propeller is the paddle stirrer with blades set at an angle of less than 90°. This might also be called a propeller stirrer with a pitch, decreasing towards the shaft. The relation between blade angle α and pitch p is given by: $\operatorname{tg} \alpha = \frac{p}{2\pi r}$, where r is the distance from the stirrer shaft.

This type of stirrer produces both an axial and a radial flow pattern. Depending on the blade angle one flow pattern will predominate. Generally, both occur, and there is therefore an axial and a radial pumping capacity: Q_{ax} and Q_{rad}. The total pumping capacity $Q = Q_{ax} + Q_{rad}$. Mixing time T can be found from $\frac{1}{T} = \frac{1}{T_{ax}} + \frac{1}{T_{rad}}$ if T_{ax} is the mixing time when only axial flow occurs, and T_{rad} the mixing time when only radial flow occurs.

The influence of blade angle α on the axial and radial (tangential) pumping capacity can be determined (theoretically) from the accompanying figure.

The relative velocity v_r between paddle and liquid is equal to the paddle velocity v_p minus velocity v_l of the liquid rotating with the stirrer (assuming that v_l has no axial or radial component). Actually the liquid velocity v_l will form an angle with the paddle velocity v_p. The relative velocity vector $\vec{v}_r$ then becomes the vector difference $v_l - v_p$ and can be split up again into the components perpendicular to and parallel to the paddle blade. It is now assumed that the momentum of the component per-

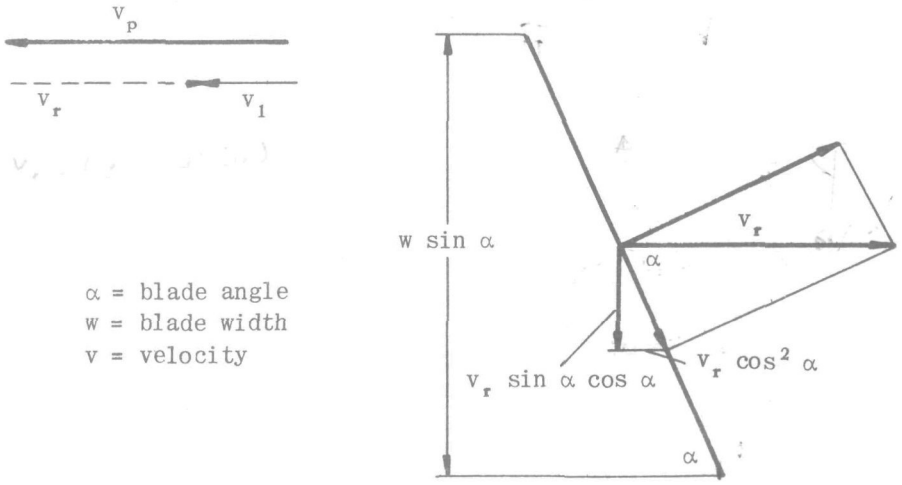

Velocity diagram for a paddle stirrer with inclined blades

pendicular to the paddle blade is destroyed. The result is then a velocity of the liquid relative to the paddle in the direction of the blade, which is equal to $v_r \cos \alpha$. The axial component becomes $v_r \cos \alpha \sin \alpha$ and the tangential component $v_r \cos^2 \alpha$. The absolute liquid velocity in tangential direction is then

$$v_p - v_r \cos^2 \alpha = v_r \sin^2 \alpha + v_1 \quad .$$

The tangential velocity is converted into a radial velocity again by centrifugal action.

Since the total liquid mass already has a tangential velocity v_1, the tangential speed relative to the surrounding liquid becomes equal to $v_r \sin^2 \alpha$ and the radial velocity which is equal to the relative tangential speed, also becomes equal to: $v_r \sin^2 \alpha$. The relative velocity v_r still depends on various factors. With an eccentric stirrer position or in the presence of baffles, v_r will be approximately equal to the paddle velocity, resulting in a maximum value of pumping capacity (see 4.1.5).

In the case, that the entire volume of liquid between the paddle blades has an axial velocity equal to $v_r \sin \alpha \cos \alpha$ and a radial velocity $v_r \sin^2 \alpha$, the axial pumping capacity becomes

$$Q_{ax} = \int_0^{\frac{1}{2}d} \omega_r (\tfrac{1}{2}d) \sin \alpha \cos \alpha \, \pi \, d \, \partial (\tfrac{1}{2}d)$$

$$= \omega_r \sin \alpha \cos \alpha \, \frac{1}{12} \pi \, d^3$$

The radial pumping capacity becomes

$$Q_{rad} = \omega_r(\tfrac{1}{2}d)\ \sin^2\alpha\ \pi dw \sin\alpha$$

$$= \tfrac{1}{2}\pi\omega_r \sin^3\alpha\ d^2w.$$

For $\alpha = 90^o$, $Q_{ax} = 0$ and $Q_{rad} = \pi^2 n_r d^2 w$.

Actually not the entire volume of liquid $\frac{\pi}{4} d^2w \sin\alpha$ will have the above-mentioned velocity, but only a part γ of that volume, which may be represented by the sector with an angle of $\gamma \times 360^o$. Then $Q_{ax} = \gamma \cdot \frac{1}{12} \pi\omega_r \sin\alpha \cos\alpha d^3$ and $Q_{rad} = \gamma \cdot \tfrac{1}{2}\pi\omega_r \sin^3\alpha d^2w$. The factor γ will be influenced by the number of blades and when this is small (1 to 3) it will be proportional to it. If we assume now that mixing time is inversely proportional to the total pumping capacity ($Q_{ax} + Q_{rad}$) and that the relative velocity v_r is proportional to the circumferential velocity of the paddle, T becomes

$$T \sim \left(\frac{1}{6}\pi^2\ n\ \gamma\ d^3 \sin\alpha \cos\alpha + \pi^2\ n\ \gamma\ d^2w \sin^3\alpha\right)^{-1}$$

Experiments were carried out with a three-bladed paddle, d being = 50 mm and w = 12 mm. The variation of T with α is then given by $T \sim (0.7 \sin\alpha \cos\alpha + \sin^3\alpha)^{-1}$. Experimental testing of this formula shows that the relation is valid for $0^o < \alpha < 60^o$ (fig. 24). In the range $60^o < \alpha < 90^o$ the experimental mixing time is seen to be shorter than that found according to the above relation.

Correlation of the mixing time with $\sin\alpha$ shows that for $40^o < \alpha < 90^o$ T is proportional to $\sin^{-2}\alpha$ (fig. 25). For smaller angles $T \sim \sin^{-1}\alpha$.

The dimensionless mixing time τ used in the correlations was finally defined as follows in the case of paddle stirrers with inclined blades:

$$\tau = \frac{Tnd^2w\ \pi^2\ \sin^k\alpha}{V} \qquad \text{(k being a function of } \alpha\text{)}.$$

allocating to $\sin^k\alpha$ the value belonging to the angle α concerned ($1 \leq k \leq 2$).

In the case of paddle stirrers with blade angle $\alpha = 90^o$, the dimensionless mixing time again reduces to the value already found, $\tau = \frac{Tnd^2w\ \pi^2}{V}$.

4.2.3. *Propeller stirrers*

The common propeller stirrer greatly resembles an ordinary ship's crew. It has screw-shaped blades with a constant pitch p. If the propeller is regarded as a paddle stirrer with blades set at an angle, we may here again derive an expression for pumping capacity, in accordance with what was found in 4.2.2. But here the blade angle α is not constant, but varies in such a manner that $\operatorname{tg} \alpha = \frac{p}{2\pi r}$, r varying from 0 (near the shaft) to ½d (extremity of stirrer blade). Now

$$\sin \alpha = \frac{p}{\sqrt{p^2 + 4\pi^2 r^2}}$$

$$\cos \alpha = \frac{2\pi r}{\sqrt{p^2 + 4\pi^2 r^2}}$$

The expression for the axial pumping capacity would become

$$Q_{ax} = \int_0^{\frac{1}{2}d} 2\pi\omega \sin\alpha \cos\alpha \, r^2 \partial r$$

$$= 4\pi^2 \omega p \int_0^{\frac{1}{2}d} \frac{r^3 \partial r}{p^2 + 4\pi^2 r^2}$$

$$= \frac{1}{8} \omega a d^3 \left\{1 - \frac{a^2}{\pi^2} \ln\left(1 + \frac{\pi^2}{a^2}\right)\right\} \quad a = \frac{p}{d}$$

For the radial pumping capacity the expression for the radial velocity is found from

$$\tfrac{1}{2} \rho v_{rad}^2 = \int_0^r \rho\omega^2 \sin^2\alpha r \partial r$$

$$= \tfrac{1}{2} \rho\omega^2 \frac{p^2}{4\pi^2} \ln\left(1 + \frac{\pi^2}{a^2}\right).$$

The radial pumping capacity then becomes

$$Q_{rad} = v_{rad} \pi d w \sin\alpha = \frac{\omega d p w}{2\sqrt{1 + \frac{\pi^2}{a^2}}} \sqrt{\ln\left(1 + \frac{\pi^2}{a^2}\right)} \qquad a = \frac{p}{d}$$

It appears from this that in spite of the rather simple flow picture on which the calculation is based, the formula for pumping capacity has already become fairly complicated. Therefore these formulae are not suitable expressions in the dimensionless mixing time of a propeller stirrer. Considering that the flow picture of a propeller stirrer is mainly axial and that it follows from the equation for Q_{ax} that $Q_{ax} \approx npd^2$, the expression $\tau = \frac{Tnpd^2}{V}$ was chosen as dimensionless mixing time. The pumping capacity of pro-

peller stirrers was experimentally determined by RUSHTON and co-workers (32). They found that under optimum conditions axial pumping capacity is directly proportional to the stirrer speed and to the square of the stirrer diameter. No proportionality to the pitch of the propeller was found. This is rather surprising, e.g. when considering the case p = 0, and in view of the results found for the power consumption of propeller stirrers (see Ch. 4.5), where the pitch has an appreciable influence.

4.2.4. *Recapitulation*

The expressions for dimensionless mixing time in their relation to stirrer type may be summarized as follows:

Type of stirrer	Flow pattern	Dimensionless mixing time ($\tau = \frac{TQth}{V}$)	Nomenclature
Paddle ($\alpha = 90^o$)	tangential	$\frac{Tnd^2w\ \pi^2}{V}$	d = stirrer diameter
Turbomixer (without deflecting blades)	radial	$\frac{Tnd^2w\ \pi^2\ \sin\beta}{V}$	w = width of blade
Paddle ($\alpha < 90^o$)	tangential and axial	$\frac{Tnd^2w\ \pi^2\ \sin^k\alpha}{V}$	β = vane angle α = blade angle
Propeller	axial	$\frac{Tnd^2p}{V}$	p = pitch

The first three formulae (paddle stirrers and turbomixer) may be classified under one general formula:

$$\tau = \frac{Tnd^2w\ \pi^2\ \sin\beta\ \sin^k\alpha}{V} \approx 7$$

which gives the mixing time for paddle stirrers (straight or inclined blades) as well as for turbomixers. This value of τ substituted in (5) gives a general formula for the mixing time, valid in the turbulent region for a vessel of appropriate size:

$$\frac{Tnd^2w\ \pi^2\ \sin\beta\ \sin^k\alpha}{V}\left(\frac{\rho n^2d^2}{\Delta\rho gH}\right)^{0.3}$$

whereas for propeller stirrers

$$\frac{Tnd^2p}{V}\left(\frac{\rho n^2d^2}{\Delta\rho gH}\right)^{0.25} \approx 9.$$

Number of blades of the stirrer

Generally, paddle and propeller stirrers have either two or three blades. In the case of turbomixers the number of blades (vanes) is usually much larger (12-20). The influence of the number of blades on pumping capacity was not extensively investigated. It was observed that experimental results correlate well when pumping capacity is taken proportional to the number of blades, at least when this is small (1, 2 or 3). When it is large, as for the turbomixer, this proportionality no longer holds; pumping capacity then approaches a maximum. The measurements with the turbomixer (12 vanes) may be brought to coincide with the results obtained with the (two-blade) paddle stirrer if pumping capacity is multiplied by a factor 2.

4.3. Vortex formation

In most cases vortexing is undesirable because then gas is dispersed into the liquid. Moreover, mixing is not further improved when the speed of the stirrer n is increased beyond the critical speed n^* at which vortex formation starts. Results of measurements on vortexing caused by centrally placed stirrers without baffles could be fitted into a correlation between a dimensionless group of Froude, viz. $\frac{n^{*2}d}{g}\frac{d}{h} = \frac{n^{*2}d^2}{gh}$ and of Reynolds' number $\frac{\rho n^* d^2}{\mu}$ (fig. 26) (h = distance between stirrer and level of liquid). For a Reynolds' number > 10^4 the quantity $\frac{n^{*2}d^2}{gh}$ proves to be constant. For low Reynolds' values (Re < 10^3) $\frac{n^{*2}d^2}{gh} \sim (\frac{\rho n^* d^2}{\mu})^{0.8}$. With the aid of these correlations the conditions to be used, when vortexing must be avoided can be calculated very simply.

4.4. Rules for scaling up

If a stirring apparatus is enlarged geometrically the conditions that have to be fulfilled to maintain the same mixing time in the large and small apparatus can be derived from eq. (5).

For

$$\mathrm{Re} > 10^3 - 10^4, \frac{Tnd^3}{D^3} \sim (\frac{\rho n^2 d^2}{\Delta\rho g H})^{-0.3}$$

(the exponent 0.3 being an average value) or $T \sim n^{-1.6}d^{-0.3}$, which means that $(nd^{0.2})$ must remain equal for T = constant. In practice this means that the number of revolutions of the stirrer

should be nearly the same in the large and small apparatus. Generally this claim will cause difficulties, as the power consumption will then become too high.

For Re < 250,

$$\frac{Tnd^3}{D^3} \sim \left(\frac{\rho n^2 d^2}{\Delta\rho g H}\right)^{-0.3} \left(\frac{\rho n d^2}{\mu}\right)^{-3}$$

or $T \sim n^{-4.6} d^{-6.3}$, which means that $(nd^{1.4})$ must remain constant for T = constant.

4.5. Power consumption

Measurement of power consumption was carried out in the same way as described in chapter 2.2.

The abundance of data given in literature on the power consumption of stirrers made it superfluous to investigate this point extensively. We therefore only measured power consumption of stirrers under conditions not yet, or not adequately, dealt with in the literature. In this way various stirring conditions on a basis of both mixing time and power consumption can be compared (Ch.5.).

The power consumption P was converted in the usual way into the dimensionless group $\frac{P}{\rho n^3 d^5}$, which was then correlated with the other dimensionless groups, such as Reynolds' number $\frac{\rho n d^2}{\mu}$ and various length ratios. These correlations are of an experimental nature. It was not found possible to establish a relationship between power consumption of the stirrer and mixing time. The two quantities are more or less independent of each other. Depending on stirring conditions, it is possible to obtain several mixing times at a given power consumption of the stirrer. Naturally, the shortest mixing time is generally to be preferred.

Paddle stirrer

A large amount of data on this type of stirrer may be found in literature. WHITE and his collaborators found the following experimental correlation (39).

$$\frac{P}{\rho n^3 d^5} \sim \left(\frac{nd^2}{\nu}\right)^{-0.14} \left(\frac{d}{D}\right)^{-1.7} \left(\frac{w}{d}\right)^{0.3} \left(\frac{H}{D}\right)^{0.6}$$

MILLER & MANN (28) found the following relations:

$$\frac{P}{\rho n^3 d^5} \sim \left(\frac{nd^2}{\nu}\right)^{-0.22} \left(\frac{H}{D}\right)^{0.66},$$

(in which only n and H were varied). This expression holds true for paddle stirrers with a blade angle of $\alpha = 90^{\circ}$, as well as for paddle stirrers with a blade angle of $\alpha = 45^{\circ}$. The proportionality constant is different in both cases.

From the survey given by HOOKER (18) it follows that

$$\frac{P}{\rho n^3 d^5} \sim \left(\frac{nd^2}{\nu}\right)^{-0.2} \left(\frac{d}{D}\right)^{-1.4} \left(\frac{H}{D}\right)^{0.62} \left(\frac{w}{D}\right)^{0.5}$$

From our own investigations we found the expression

$$\frac{P}{\rho n^3 d^5} \sim \left(\frac{nd^2}{\nu}\right)^{-0.15} \left(\frac{d}{D}\right)^{-1.3} \qquad \text{(fig. 27, 29)}$$

The influence of $\frac{H}{D}$ and $\frac{w}{d}$ was not further examined as these quantities have already been sufficiently ascertained. So, the following formula may be used with fairly considerable reliability for the power consumption of paddle stirrers:

$$\frac{P}{\rho n^3 d^5} \sim \left(\frac{nd^2}{\nu}\right)^{-0.15} \left(\frac{d}{D}\right)^{-1.3} \left(\frac{H}{D}\right)^{0.6} \left(\frac{w}{d}\right)^{0.4} \qquad (6)$$

These formulae only apply in the turbulent region, i.e. for $Re > 10^3$ to 10^5.

For $Re < 10^2$ to 10^3 the flow becomes laminar, as was found already in the measurements of mixing time. In this region

$$\frac{P}{\rho n^3 d^5} \sim \left(\frac{nd^2}{\nu}\right)^{-1}$$

T u r b o m i x e r s

The relations valid for paddle stirrers also apply in the case of turbomixers.

For turbomixers MACK gives the following complicated relation in the turbulent region (26)

$$\frac{P}{\rho n^3 d^5} = 9.74\ s^{0.495} \left(\frac{w}{d}\right)^{1.33\ s^{-0.108}}$$

For practical use the formula may be simplified to

$$\frac{P}{\rho n^3 d^5} = 9.7\ s^{0.5} \left(\frac{w}{d}\right)^{1} \qquad (s = \text{number of vanes})$$

The influence of Reynolds' number was negligible owing to the presence of stator rings.

To ascertain what happens to the power consumption when the paddle stirrer is changed into a turbomixer the influence of vane angle β on power consumption was measured. The relation can be represented by the formula

$$\frac{P}{\rho n^3 d^5} \sim (\sin \beta)^{0.23} \qquad \text{(table XIVa)}$$

This relation was ascertained for the turbulent region.

Propeller stirrers and paddle stirrers with inclined blades ($\alpha < 90^{o}$)

The formula (6) is also more or less applicable to propeller stirrers.

Measurements by STOOPS and LOVELL (33) produced the following result:

$$\frac{P}{\rho n^3 d^5} \sim \left(\frac{nd^2}{\nu}\right)^{-0.2} \left(\frac{d}{D}\right)^{-0.9}$$

(in these measurements only n and d were varied).

The diameter remaining the same, power consumption increases about proportionately to the pitch of the propeller (31). Only few reliable measurements on this point are recorded. For paddle stirrers the influence of blade angle α on power consumptuon was ascertained (fig. 28). It is found that

$$\frac{P}{\rho n^3 d^5} \sim (\sin \alpha)^{\simeq 2.5}$$

The relation between power consumption and Reynolds' number is shown in fig. 29. It is in fair agreement with that for propellers, as given by RUSHTON (31). No baffles were used with all these experiments.

Baffling, eccentricity of stirrer

If the mixing vessel is fitted with baffles (see fig. 2a), or in case of a turbomixer with a stator ring round the turbine wheel, the influence of Reynolds' number on the power number is practically absent. Power consumption increases by a factor 2 to 5 (fig. 30), when using baffles.

Eccentricity of the stirrer has about the same effect on power consumption as has baffling. Measurements on paddle stirrers showed an increase in power consumption by a factor 1.5 to 2.5, this increase being 1 to 1.5 in the case of propeller stirrers ($e = 0.5$).

5. DISCUSSION OF OPTIMUM STIRRING CONDITIONS

5.1. Conditions for optimum performance (efficiency)

With the correlations found for mixing time and power consumption optimum conditions may be derived for the dimensions and shape of the stirrer and vessel.

The optimum stirring condition may be defined in several ways, e.g.

a) the condition at which the power consumption is lowest for a specified mixing time.
b) the condition at which the mixing time is shortest for a specified power consumption.

The analysis of the data will be made according to the first definition of optimum conditions. However, we mention that an analysis based on the second definition in most cases leads to the same results.

For a given mixing process the physical properties of the liquid are, of course, fixed. The shape and dimensions of the stirrer and vessel are generally, within certain limits, left to the designer. When these variables, too, have been decided upon, the speed of rotation must be such as to ensure mixing within the required time.

For the mixing time T we may write

$$T = T\left(n, \frac{d}{D}, V, \frac{H}{D}, \frac{w}{d}, \alpha, \beta\right)$$

and for power consumption P

$$P = P\left(n, \frac{d}{D}, V, \frac{H}{D}, \frac{w}{d}, \alpha, \beta\right).$$

Successively, we shall now deal with the influence of the liquid volume V in the mixing vessel;

the stirrer diameter ratio $\frac{d}{D}$;

the height of the liquid in the vessel $\frac{H}{D}$;

the width of the stirrer blade $\frac{w}{d}$;

blade angle α;

vane angle β.

The procedure used in order to determine optimum conditions

consists in varying n and only one of the other variables, the remaining ones being kept constant. For constant mixing time the variation of n depends on the variation of this one variable. Now, in various cases, that value of the variable may be determined at which the power consumption is lowest.

In this way optimum values may be established for all variables involved. Because of the special structure of the formulae for T and P the optimum value found for one variable holds true for quite considerable changes of the other variables.

5.2. Influence of liquid volume to be mixed

If $\tau \sim \left(\frac{\rho n^2 d^2}{\Delta\rho g H}\right)^{-0.3}$ and further T does not depend on the Reynolds' number then equation (5) may be written as

$$T \sim n^{-1}(n^2 d)^{-0.3}$$

while equation (6) becomes $P \sim n^3 d^5 (nd^2)^{-0.15}$.

Elimination of n gives

$$P \sim T^{-1.78}\, d^{4.17}$$

or

$$P \sim T^{-1.78}\, V^{1.4} \qquad (\text{as } d^3 \sim V)$$

Power consumption per unit volume, $\frac{P}{V}$, is proportional to $T^{-1.78}V^{0.4}$ and therefore increases when the liquid volume increases (no optimum). The mixing energy per unit volume, $\frac{PT}{V}$, which is proportional to $T^{-0.78}\, V^{0.4}$, also increases at higher V values as well as at smaller T values.

When the quantity $\frac{\rho n^2 d^2}{\Delta\rho g H}$ has no influence on τ, $P \sim T^{-2.85}V^{1.6}$ and therefore $\frac{PT}{V} \sim T^{-1.85}V^{0.6}$. It is therefore advantageous to use a small "mixing volume". In large vessels several small stirrers which are pumping in the same direction are to be preferred to one large stirrer.

5.3. Influence of stirrer and vessel dimensions

5.3.1. *Influence of the stirrer/vessel diameter ratio* $\frac{d}{D}$ ($\frac{H}{D}$ and D^2H are constant)

The equation for T becomes:

$$T \sim n^{-1.6}\, d^{-3.6}\, f\left(\frac{d^3}{D^{2.5}H^{0.5}}\right) \qquad (Re > 10^4)$$

where $f\left(\frac{d^3}{D^{2.5}H^{0.5}}\right)$ is given by fig. 20, and equation (6) becomes

$$P \sim n^{2.85}\, d^{4.4} \left(\frac{d}{D}\right)^{-1.3} .$$

For $\frac{d^3}{D^{2.5}H^{0.5}} < 0.04$, $f\left(\frac{d^3}{D^{2.5}H^{0.5}}\right)$ = constant. For the mixing time T it is then true that $T \sim n^{-1.6}\, d^{-3.6}$. Furthermore, $P \sim n^{2.85}\, d^{3.1}$. Elimination of n produces $P \sim T^{-1.78}\, d^{-3.4}$. For a given time T, the power consumption will decrease as stirrer diameter increases. It is therefore best to take the largest possible diameter. For $\frac{d^3}{D^{2.5}H^{0.5}} > 0.08$ it is true that $f\left(\frac{d^3}{D^{2.5}H^{0.5}}\right) \sim \frac{d^3}{D^{2.5}H^{0.5}}$. The mixing time T becomes

$$T \sim n^{-1.6}\, d^{-3.6} \left(\frac{d}{D}\right)^3 \qquad \text{or} \qquad T \sim n^{-1.6}\, d^{-0.6}$$

and

$$P \sim n^{2.85}\, d^{4.4} \left(\frac{d}{D}\right)^{-1.3} .$$

Elimination of n produces:

$$P \sim T^{-1.78}\, d^{3.4} \left(\frac{d}{D}\right)^{-1.3} \qquad \text{or} \qquad P \sim T^{-1.78}\, d^{2.0} .$$

In this region P will increase with increasing stirrer diameter if T is kept constant. It is then best to keep stirrer diameter as small as possible.

There is therefore an optimum diameter in the region

$$0.04 < \frac{d^3}{D^{2.5}H^{0.5}} < 0.08 \qquad \text{or} \qquad 0.34 < \left(\frac{d}{D}\right)\left(\frac{D}{H}\right)^{1/6} < 0.43$$

This practically means that this diameter corresponds with a value of $\frac{d}{D} \approx 0.4$, as the value of $\left(\frac{D}{H}\right)^{1/6}$ in most cases does not deviate very much from 1.

The above results are only valid for a turbulent field of flow. In the laminar range (Re < 250) mixing time very rapidly increases at lower Reynolds' values (figures 18 and 19). In this case it is better to take the largest possible stirrer diameter, as will be shown below. In this region it has been assumed that:

$$\frac{Tnd^3}{V}\left(\frac{\rho n^2 d^2}{\Delta\rho g H}\right)^{0.3} \sim \left(\frac{\rho n d^2}{\mu}\right)^{-3} \cdot f\left(\frac{d^3}{D^{2.5}H^{0.5}}\right)$$

and

$$\frac{P}{\rho n^3 d^5} \sim \left(\frac{nd^2}{\nu}\right)^{-1} \cdot \left(\frac{d}{D}\right)^{-1.3} .$$

If $f\left(\frac{d^3}{D^{2.5}H^{0.5}}\right) = \left(\frac{d}{D}\right)^3$ (for $\frac{d^3}{D^{2.5}H^{0.5}} > 0.08$ and $\frac{H}{D}$ = constant). we find

$$P \sim T^{-0.44}\, d^{-1.1} ,$$

which proves that a large diameter is favourable here. In actual practice the stirrer diameter will have to be about equal to the vessel diameter when mixing viscous liquids.

5.3.2. *Influence of liquid height* $\frac{H}{D}$ ($\frac{d}{D}$ and D^2H are constant)

In the same way as shown in the preceding paragraph the influence of $\frac{H}{D}$ can also be ascertained. From equation (5) it follows that $T \sim n^{-1}\, d^{-3} \left(\frac{n^2 d^2}{H}\right)^{-0.3} f\left(\frac{H}{D}\right)$, while from equation (6) it is found that $P \sim n^3 d^5 (nd^2)^{-0.15} \left(\frac{H}{D}\right)^{0.6}$. Elimination of n now ($D^2H$ is constant) gives the following relation: $P \sim T^{-1.8} H^{1.22} \{f\left(\frac{H}{D}\right)\}^{1.8}$. For $\frac{d^3}{D^{2.5}H^{0.5}} < 0.05$, $f\left(\frac{H}{D}\right)$ = constant, so that then $P \sim T^{-1.8} H^{1.22}$. In other words P increases with increasing H values.

For $\frac{d^3}{D^{2.5}H^{0.5}} > 0.05$, $f\left(\frac{H}{D}\right) = \left(\frac{H}{D}\right)^{-0.5}$ and as $D \sim H^{-0.5}$, $P \sim T^{-1.8} H^{1.22-1.35} = T^{-1.8} H^{-0.13}$. So in this region P slightly decreases with increasing H values. There is therefore an optimum value for $\frac{d^3}{D^{2.5}H^{0.5}} = 0.05$. When $\frac{d}{D}$ is taken equal to 0.4 the value for $\frac{H}{D}$ proves to become ≈ 0.8, which is a normal charge depth in actual practice.

5.3.3. *Width of stirrer blade (influence of* $\frac{w}{d}$)

From the formula for power consumption and mixing time, giving the influence of the width of the stirrer, we may derive rules for the most favourable dimensions of the stirrer.

From eq. (6) it can be derived that $\frac{P}{\rho n^3 d^5} \sim \left(\frac{w}{d}\right)^{0.4}$, while $T \sim (nd^2w)^{-1}$ holds good (if $\frac{w}{d} < 0.5$) (table IX), when the Froude number has no influence. Elimination of n gives $P \sim T^{-3} w^{-2.6}$. Therefore $P \sim w^{-2.6}$ for T = constant.

According to this formula it is therefore best to have the widest possible blade.

For values of $\frac{w}{d} > 0.5$, $T \sim (nd^2w)^{-1} \left(\frac{w}{d}\right)^{0.66}$ (table IX) is val-

id, therefore $T \sim n^{-1}\ w^{-0.33}$. For power consumption P, we then find, after elimination of n: $P \sim T^{-3}\ w^{-0.6}$.

So for $\frac{w}{d} > 0.5$, there is still a small effect of $\frac{w}{d}$ on the efficiency. In practice the ratio $\frac{w}{d} = 0.5$ is never exceeded.

In the case that the density Froude number is of influence we get for

$$\frac{w}{d} < 0.5 \qquad P \sim T^{-1.9}\ w^{-1.5}$$

$$\frac{w}{d} > 0.5 \qquad P \sim T^{-1.9}\ w^{-0.2}$$

i.e. the trend remains the same.

5.4. Type of the stirrer

5.4.1. *Influence of blade angle* α

The value of blade angle α more or less determines the type of stirrer (paddle or propeller), and the influence of α shows what type of stirrer is the most effective. From the relation found between mixing time and blade angle it can be ascertained what blade angle is the most suitable.

$$T \sim n^{-1.6}\ (\sin \alpha)^{-k_1} \qquad k_1 = 1 \text{ to } 2.$$

$$P \sim n^{2.85}\ (\sin \alpha)^{k_2} \qquad k_2 = 2 \text{ to } 3.$$

Elimination of n produces

$$P \sim T^{-1.78}\ (\sin \alpha)^{k_2 - 1.7\ k_1}$$

For constant mixing time T, P varies according to

$$P \sim (\sin \alpha)^{k_2 - 1.7\ k_1}$$

For $(k_2 - 1.7\ k_1) > 0$, P increases with $\sin \alpha$; for $(k_2 - 1.7\ k_1) > 0$ it decreases with $\sin \alpha$. From figs. 25 and 28 the k_2 and k_1 values for various values of α may be found.

For $0^o \leq \alpha \leq 45^o$, $k_1 \approx 1$ and $k_2 \approx 1.5$, so that $k_2 - 1.7\ k_1 \sim -0.2$. For $45^o \leq \alpha \leq 90^o$, $k_1 \approx 2$ and $k_2 \approx 2.4$; then $k_2 - 1.7\ k_1 \sim 0$.

The small values found for $k_2 - 1.7\ k_1$ make it clear that the influence of α is only very small, in other words the propeller stirrer has about the same performance as the paddle stirrer.

5.4.2. *Influence of vane angle* β

The influence of the vane angle decides whether a paddle ($\beta = 90^{o}$) or a turbomixer ($\beta < 90^{o}$) is to be preferred. The equation for mixing time in this case becomes

$$T \sim n^{-1.6} (\sin \beta)^{-1}$$

and the equation for power consumption

$$P \sim n^{2.85} (\sin \beta)^{0.23}.$$

Therefore $P \sim T^{-1.8} \sin \beta^{-1.6}$.

Hence, for mixing a high sin β value is favourable, in other words the paddle mixer is more efficient than the turbomixer.

5.5. Comparison with jet mixing

Jet mixing with external circulation of liquid is much applied in industry. An important point is the size of the nozzle. FOSSETT and PROSSER (10) investigated the possibilities of jet mixing and derived an expression for the mixing time. This enables us to compare jet mixing with mixing by agitation, by extrapolation the large scale results of FOSSETT and PROSSER to our small scale experiments. The basis of comparison is again power consumption with equal mixing time (see fig. 31).

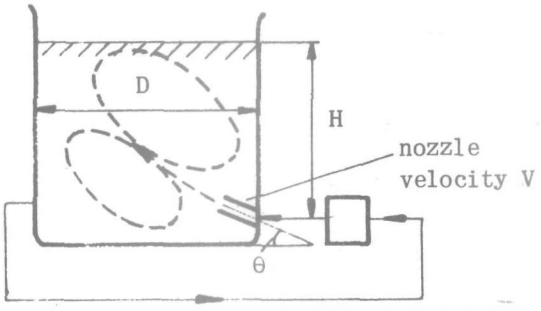

The velocity of the liquid v at the nozzle must comply with the condition $\frac{v^2}{2g} = k \frac{H (\rho_2 - \rho_1)}{\rho_2 \sin^2 \theta}$ (10) in which k is a constant still dependent on $\frac{\rho_2 - \rho_1}{\rho_2}$ [$k \sim (\frac{\rho_2 - \rho_1}{\rho_2})^{-0.3}$]. For $\frac{\rho_2 - \rho_1}{\rho_2}$ = 0.079, k = 14, H = 118 mm. Take sin θ to be $\frac{1}{2}\sqrt{2}$, then $\frac{v^2}{2g}$ =

0.26 m and v = 2.30 m/sec. The mixing time T can be found from $T = \frac{8D^2}{\sqrt{Qv}}$. For D = 148 mm T becomes $T = 0.120\ Q^{-0.5}$ sec. (Q in m^3/sec.).

The required power input is found from $P = \frac{1}{2} \rho v^2 \times Q = 2.6 \times 10^{+3}\ Q$ Nm/sec. Fig. 31 gives the P and T values corresponding to various Q values. It is seen that the power consumption in jet mixing is about four times as great as in paddle mixing and about the same as in the cone stirrer. Elimination of Q gives $PT^2 = 37.5$ Nm sec.

5.6. Comparison with the cone stirrer

Since the pumping action of the cone stirrer is brought about by quite a different mechanism, it is not possible by gradually changing one variable to determine the merits of the cone stirrer as compared with the types of stirrer dealt with above. But they may be compared with the aid of fig. 31, where the power consumption per unit of volume is plotted against mixing time for the cone stirrer and a paddle stirrer of the same diameter and under the same stirring conditions whenever possible. It is seen that for T = constant the cone stirrer needs three to four times the power consumption of the paddle stirrer. Moreover, the rotational speed of the cone stirrer for T = constant is a factor four times as large as that of the paddle stirrer, which is often a disadvantage in practice.

5.7. Concluding remarks

A general survey of the efficiency of the various types of stirrers, using the optimum stirrer dimensions, is represented in the following table.

Comparison between some types of stirrer on a basis of power consumption (in arbitrary units) required to ensure a certain mixing time T			Optimum dimensions of stirrer
Paddle stirrer	no baffles	100	V as small as possible
Turboxixer	no baffles	170	$\frac{d}{D} = 0.4$
Propeller stirrer	no baffles	100	$\frac{H}{D} = 0.8$
Cone stirrer		360	$\frac{w}{d} = 0.5$
Jet mixing		400	$\beta = 90^o$

6. CONTINUOUS MIXING OF LIQUIDS

6.1. Introduction

By continuous mixing of liquids will be meant the operation where one or more streams of liquid are continuously fed into and discharged from a mixing vessel. Both the flow rates and the compositions of the entering liquids may vary with time. The flow rate at the outlet will at any time be equal to the sum of the flow rates of the entering streams; the final composition will be a function of the flow rates and compositions of the entering liquids and of the degree of mixing in the mixing vessel.

Mixing in the mixing vessel is called perfect (one idel mixing stage) if the entering liquids are immediately and completely mixed with the fluid in the vessel, so that its properties are uniform and identical with those of the outgoing stream. This case is frequently encountered in the literature and calculations on stirred reactors are often based on this assumption.

Complete absence of mixing is occurring, if the elements of the entering liquid move through the vessel with constant and equal velocities along parallel paths, so that no mixing takes place either in the direction of flow or in other (radial) directions. The case of no mixing in the directions of flow (perfect piston flow) can be approached by an infinite number of ideal mixing stages lined up in series.

The normal case of a non-perfect mixer is very difficult to handle mathematically. The conception of an eddy diffusivity in axial and (or) in radial direction, as usually applied in packed beds and in particulate fluidized beds, does not hold for the case of an agitated vessel.

The continuous-flow mixing of one liquid stream can be suitably characterized by the curve of the outlet concentration against time if the inlet concentration is a well-defined function of time (e.g. a step function).

In many processes two liquid streams with constant concentrations must be mixed. In this particular case only mixing in a radial direction is important which can be effected, for instance, by line blending. As a rule the liquid will be uniform after having passed through a pipe length of about thirty times the pipe diameter (turbulent flow conditions). Bends and constrictions appreciably improve mixing.

To conclude with our investigation, a few experiments were

performed with one liquid stream to evaluate the relation between batch mixing and continuous mixing.

6.2. Measurements (mixing times)

The experiments were carried out in a mixing vessel (H = D = = 0.15 m) with a centrally placed stirrer (fig. 35 A). In order to obtain an even distribution of the entering liquid stream the vessel was provided with an inlet compartment consisting of perforated plates with the same diameter as the vessel. In this way mixing in the direction of flow caused by the injection of the fluids was suppressed. Disturbance of the flow pattern by the outlet was avoided by the use of a sieve bottom.

As this investigation only aimed at the study of stirrers, the influence of different types of inlet nozzles, etc., was not further examined.

A small amount of dye solution (bromophenol blue) was instantaneously injected into the entering liquid stream (10 ml in 1 sec.). The distribution of the colour through the mixing vessel and in the outgoing streams (under the sieve bottoms) was watched. The outlet concentration curves for a perfect mixer and a piston flow mixer are given in fig. 35b (curves 1 and 2).

The outlet concentration will show a maximum, which in the normal case of a non-perfect mixer will appear a time T after the moment of dye injection, which time is shorter than the average residence time ($\frac{\text{volume of vessel}}{\text{flow rate}}$) (fig. 35b curve 3).

In most cases some time after the injection an even colour distribution throughout the vessel could be observed (6), which time corresponds with the time T. The piston flow mixer (fig. 35b, curve 2) will of course never give such a mixing time. Mixing times T were measured as a function of agitator speed and flow rate. The influence of the flow rate on T in the case of a stagnant stirrer is shown in fig. 34. The times then found (called T_2) are always shorter than the residence times (T_R).

The value of $\frac{T_2}{T_R}$ will, of course, depend on the conditions of flow in the mixing vessel, hence on the construction of the inlet, chanelling effects, etc.

The influence of the stirrer speed on the mixing time T when there is no flow, is shown in fig. 33. This mixing time T_1 is the same as the mixing time obtained for batch mixing, as discussed in the previous chapters of this thesis. In the case of both liquid flow and stirring the mixing times T appear to correlate with

the batch mixing time T_1 and the time T_2, as is shown in fig. 32. The best correlation for T in terms of T_1 and T_2 is given by

$$\frac{1}{T} = \frac{1}{T_1} + \frac{1}{T_2} + \frac{0.5}{\sqrt{T_1 T_2}} .$$

Summarizing our results it may be stated that in the case of continuous flow through a stirred vessel the mixing time T can be predicted from the mixing time in batch operation (T_1) and a time T_2, which is always shorter than the residence time.

If the batch mixing time $T_1 \ll T_R$, then $T \ll T_R$, in which case a perfect mixer is approached.

LIST OF SYMBOLS

	Units
d = stirrer diameter	m
D = vessel diameter	m
e = eccentricity of stirrer	–
F = force	N
g = acceleration of gravity	m/sec^2
H = height of liquid in vessel	m
l = length of cone (cone stirrer)	m
n = number of revolutions of stirrer	sec^{-1}
n_D = refractive index	
p = pitch of propeller stirrer	m
P = power consumption	Nm/sec
Q = pumping capacity	m^3/sec
r = radius	m
s = number of vanes (or blades)	–
s = slit width (cone stirrer)	m
T = mixing time	sec
v = velocity	m/sec
V = liquid volume in mixing vessel	m^3
W = work per unit mass	m^2/sec^2
w = width of stirrer blade	m

	Units
α = blade angle (paddle with inclined blades)	–
β = vane angle (turbomixer)	–
δ = boundary layer (cone stirrer)	m
μ = dynamic viscosity of liquid	$Nsec/m^2$
ν = kinematic viscosity of liquid	m^2/sec
ρ = density of liquid	kg/m^3
ω = angular velocity	sec^{-1}
$\tau = \frac{TQ_{th}}{V}$ = dimensionless mixing time	–
$\frac{\rho n^2 d^2}{\Delta\rho g H}$ = density Froude number	–
$\frac{\rho n d^2}{\mu}$ = Reynolds' number	–
$\frac{d^3}{D^{2.5} H^{0.5}}$ = dimensionless group, comparing the dimensions of the stirrer and the dimensions of the mixing vessel	–
$\frac{P}{\rho n^3 d^5}$ = dimensionless power consumption	–

REFERENCES

1. W. L. Badger, J. C. Wood, E. R. Whittemore, — Chem. Met. Eng. **27**, 1176, 1922
2. E. Brunner — Z. physik. Chem. A **47**, 56, 190, 1904, **51**, 95, 494, 1905
3. W. Büche — Z. Ver. Deut. Ing. **81**, 1065, 1937
4. T. H. Chilton, T. B. Drew, R. H. Jebens — Ind. Eng. Chem. **36**, 510, 1944
5. L. E. J. Dodd — J. Phys. Chem. **31**, 1761, 1927
6. R. W. McDonald, E. L. Piret — Chem. Eng. Progress **47**, 363, 1951
* 7. R. Erdmenger, S. Neidhardt — Chem. Ing. Techn. **24**, 248, 1952
8. A. Fage — Proc. Roy. Soc. (London) **165**, 513, 1938
9. H. O. Forrest, B. E. Roetheli, R. H. Brown, — Ind. Eng. Chem. **23**, 650, 1931
10. H. Fossett, L. E. Prosser — Proc. Inst. Mech. Engrs. **160**, 224, 1949
11. S. Goldstein — Modern developments in fluid dynamics, Oxford, 1938
12. W. Heller — Z. physik. Chem. A. 431, 1929
13. J. Hill — Chem. Met. Eng. **28**, 1077, 1923
14. A. W. Hixson, S. J. Baum — Ind. Eng. Chem. **33**, 478, 1433, 1946
    Ind. Eng. Chem. **34**, 120, 194, 1942
15. A. W. Hixson, A. H. Tenney — Trans. Am. Inst. Chem. Engrs. **31**, 113, 1935
16. A. W. Hixson, M. J. Smith — Ind. Eng. Chem. **41**, 973, 1949
* 17. A. W. Hixson — Ind. Eng. Chem. **36**, 488, 1944
* 18. T. Hooker — Chem. Eng. Progress **44**, 833, 1948
19. C. V. King — J. Am. Chem. Soc. **57**, 828, 1935
20. C. V. King, P. L. Howard — Ind. Eng. Chem. **29**, 75, 1937
21. H. Kramers, W. H. Knoll — Ingenieur **63**, Ch 9, 67, 1951
22. H. Kramers, G. M. Baars, W. H. Knoll — Chem. Eng. Sci. **2**, 35, 1953

23. H. Kraussold — Chem. Ing. Techn. **23**, 177, 1951

* 24. D. W. van Krevelen, J. Huiskamp — Ingenieur **61**, Ch 6, 15, 1949

25. G. McLean, E. F. Lyons — Ind. Eng. Chem. **30**, 489, 1938

26. D. E. Mack — Chem. Eng. **47**, 109, 1951

27. E. M. Mack, R. E. Marriner — Chem. Eng. Progress **45**, 545, 1949

28. S. A. Miller, Ch. A. Mann — Trans. Am. Inst. Chem. Engrs. **40**, 709, 1944

29. W. Möhle — Chem. Ing. Techn. **21**, 335, 1949 **24**, 495, 1952

30. W. Nernst — Z. physik. Chem. **15**, 148, 1904

31. J. H. Rushton — Chem. Eng. Progress **46**, 470, 1950

32. J. H. Rushton, D. E. Mack, H. J. Everett — Trans. Am. Inst. Chem. Engrs. **42**, 441, 1946

33. C. E. Stoops, C. L. Lovell — Ind. Eng. Chem. **35**, 845, 1943

34. H. Schardin — Ergebnisse der exakten Naturwissenschaften **20**, 304, 1942

35. G. I. Taylor — Proc. Roy. Soc. (London) **A 102**, 541, 1923

36. G. I. Taylor — Proc. Roy. Soc. (London) **A 151**, 494, 1935

37. G. I. Taylor — Proc. Roy. Soc. (London) **A 157**, 546, 1935

38. F. A. Wattendorf — Proc. Roy. Soc. (London) **148**, 565, 1935

39. A. M. L. White, E. Brenner — Trans. Am. Inst. Chem. Engrs. **30**, 585, 1934

40. A. M. L. White, S. D. Sumerford — Chem. Met. Eng. **43**, 370, 1936

41. A. M. L. White, S. D. Sumerford, E. O. Bryant, B. E. Lukens — Ind. Eng. Chem. **24**, 1160, 1932

* Surveys

Table I

Influence of $\Delta\rho$ and n_D^{20} on mixing time

Mixing experiments with water, acetic acid and dilutions of acetic acid (cone stirrer)

Speed r.p.m.	Difference in density $\Delta\rho$ in kg/m^3	Difference in refractive index n_D^{20}	Mixing time T in sec.
178	36.1	0.03995	1560
434	36.1	0.01825	38.4
390	36.1	0.00955	29.4
437	18.6	0.00955	24.8
437	18.6	0.00955	25.0
440	9.4	0.00485	19.8
435	9.4	0.00485	20.0
439	5.6	0.00245	17.0
439	5.6	0.00245	16.6
439	2.3	0.00125	13.2
414	2.3	0.00125	14.8
429	2.3	0.00125	14.0
437	1.1	0.00055	13.2
430	1.1	0.00055	13.2
438	0.6	0.00025	11.2
430	0.6	0.00025	14.8
438	56.0	0.0397	77.4
438	56.0	0.0397	76.0
437	58.2	0.0327	56.2
438	58.2	0.0327	59.6
430	69.5	0.0419	79.4
443	69.5	0.0419	68.6
443	47.3	0.0259	42.2
432	47.3	0.0259	42.0
440	26.6	0.0141	29.6
437	26.6	0.0141	29.4
440	66.0	0.0372	58.8
437	66.0	0.0372	62.2
437	40.5	0.0254	37.4
438	40.5	0.0254	37.2
436	21.8	0.0113	25.8
440	21.8	0.0113	26.0
442	49.7	0.0272	43.4
440	49.7	0.0272	46.2
436	28.3	0.0148	31.0
434	28.3	0.0148	31.4
433	51.7	0.0314	57.0
432	51.7	0.0314	52.6

Table I (continued)

Speed r.p.m.	Difference in density $\Delta\rho$ in kg/m^3	Difference in refractive index n_D^{20}	Mixing time T in sec.	
438	33.2	0.0188	32.8	
437	33.2	0.0188	33.2	
433	13.9	0.0085	21.2	
433	18.8	0.0102	23.4	
438	18.8	0.0102	23.2	
434	11.0	0.0053	18.8	
437	11.0	0.0053	19.2	
437	4.9	0.0025	14.8	
432	5.5	0.0026	14.0	
436	5.5	0.0026	15.6	
436	21.6	0.0112	25.6	
440	18.4	0.0140	26.0	
440	18.4	0.0140	22.2	
438	43.1	0.0155	38.8	
440	44.1	0.0155	40.4	
439	18.5	0.0110	24.6	
440	4.0	0.0284	20.8	acetic
440	4.0	0.0284	20.4	acid and
440	6.1	0.0284	17.8	ethanol
438	7.0	0.0160	19.4	dilutions
438	7.0	0.0160	18.8	

Table II

Influence of stirrer speed on mixing time
Water-glycerin-glycerin dilutions (cone stirrer)

Speed r.p.m.	Difference in density $\Delta\rho$ in kg/cm^3	Mixing time in sec.
600	73.8	31.2
612		29.0
512		42.2
501		45.0
422		64.6
420		74.4
326		180
326		165
226		600
227		600
620	38.2	16.6
620		17.2
524		23.8
530		23.2
422		39.6
428		37.4
326		70.0
329		68.6
225		260
226		240
225	19.4	100
228		100
326		39.6
322		41.4
416		24.2
419		25.4
517		18.2
522		17.8
617		14.0
625		13.2
330	9.9	27.2
328		25.8
226		57.8
227		55.2
243		50.4
266		44.4

Table II (continued)

Speed r.p.m.	Difference in density $\Delta\rho$ in kg/m^3	Mixing time in sec.
267	9.9	42.2
265	41.0	150
266		135
327		74
331		75.8
226	24.1	140
228		133
267		75
266		85
266		98
770	75.6	17.6
740		19.6
1250		8.2
1200		8.0
1750		6.6
1880		5.0
1180	155.4	13.0
1100		13.0
1940		5.8
1930		5.8
2540		3.6
2575		3.8
2540	602	4.6
2480		5.0
2100		6.4
1800		6.6
1190		21.0
1120		24.4
3520		2.6
5200		1.8
3750		2.4

Table III

Influence of viscosity on mixing time (cone stirrer)

Speed r.p.m.	Difference in density $\Delta\rho$ in kg/m^3	Viscosity of top layer in 10^{-3} N sec/m^2 (= c Poise)	Final viscosity in 10^{-3} N sec/m^2 (= c Poise)	Mixing time in sec.
430	74.0	0.911	1.4	59.0
433				61.0
433	38.5	0.899	1.1	35.2
431				34.4
430	19.4	0.915	1.05	23.2
433				23.2
428	38.6	64.3	178	ca 200
414				ca 200
421	11.0	45	55	ca 50
422	14.2	8.9	10.1	29.0
420				32.6
418	105.8	2.8	6.0	90.6
421				100
425	48.8	3.9	6.1	34.6
428				37.4
600	108.7	2.2	5.5	35.8
620				32.0
627	94.1	5.5	18	31.4
620				30.6
625	20.9	18	27	20.0
614		18	27	22.4
938	39.3	66	180	ca 120
1980		66		ca 35
1900	19.4	180	340	ca 40
2150		180		ca 20
3035		180		15
2077	38.7	32	72	8.2
998				ca 50
1000	40.1	10.2	18	17.0
2085				5.2

Table IV

Influence of volume ratio between two liquid layers (cone stirrer)
(total volume 2.10^{-3} m^3)

Speed r.p.m.	Difference in density $\Delta\rho$ in kg/m^3	Volume bottom layer in 10^{-6} m^3	Mixing time in sec.
326	37.4	200	25.0
330		200	27.2
329		400	37.6
330		400	35.4
329		600	53.2
330		600	52.6
330		800	67.0
328		800	65.2
329		1200	76.0
329		1200	79.8
329		1400	73.6
329		1400	76.8
328	37.8	1600	73.0
330		1600	71.4
325		1800	61.8
329		1800	70.2
326	19.7	1800	42.4
327		1800	40.6
329		1600	41.2
328		1600	43.4
329	19.9	1400	46.6
330	19.7	1400	46.0
329	19.9	1200	44.2
328		1200	49.0
327		800	41.0
327		800	42.4
326		600	35.8
328		600	33.6
328		1900	ca 34
330		1000	42.8
326		200	23.4

Table V

Influence of slit width on mixing time (cone stirrer)

Speed r.p.m.	Slid width mm	Difference in density $\Delta\rho$ in kg/m^3	Mixing time in sec.	Pumping capacity in in 10^{-6} m^3/sec.	
430	6.5	82.8	72	23.5	
325	6.5	82.8	ca 150	11.9	
328	6.5	82.8	ca 155	11.9	
266	6.5	40.7	ca 140	11.8	
266	6.5	40.7	136	11.8	
264	6.5	40.7	102	16.7	
266	6.5	40.7	100	16.7	
430	6.5	39.7	41.4	38.6	
430	6.5	39.7	40.0	38.6	
430	4.4	39.7	45.6	38.6	
431	4.4	39.7	46.0	38.6	
429	3.1	39.7	62.2	34.8	
425	2.1	39.7	90.6	32.8	
429	2.1	39.7	97.0	32.8	
423	1.64	39.7	159	24.6	
431	1.64	39.7	151	24.6	
428	1	39.7	ca 300	15.6	
431	1	39.7	ca 300	15.6	
432	0.8	39.7	ca 380	10.1	
431	0.8	39.7	ca 380	10.1	
327	5.5	39.5	88.6	22.0	
266	5.5	39.5	171	12.7	
430	1.64	39.5	58.4	26.4	
430	1.64	39.5	62.4	26.4	
1410	4.5	75.9	7.4	163	
1430	4.5	75.9	7.0	163	
1440	4.5	75.9	7.6	163	
1450	2.1	75.9	11.0	131	
1400	2.1	75.9	11.4	131	
1400	1	75.9	26.4	65	
1450	1	75.9	23.0	65	
1420	6	75.9	52.8	33	
1450	6	75.9	73.9	33	
1360	6.5	75.9	7.6	183	
1420	3.5	75.9	8.0	153	
1380	3.5	75.9	9.0	153	
624	6.5	39.0	ca 250	112.5	in 0.02m^3 vessel 0.26 m diam.
430	6.5	19.7	ca 440	71.5	
625	6.5	20.5	ca 166	13.2	
631	3.5	40.7	15.6	98	
630	3.5	40.7	15.4	98	length of inner cone 50 mm
266	3.5	40.7	ca 100	17.6	
266	3.5	40.7	113	17.6	
265	3.5	40.7	65.4	33.6	
265	3.5	40.7	68.6	33.6	

Table VI

Power consumption as a function of stirrer speed (cone stirrer)

Speed r.p.m.	Power consumption in 10^{-4} N m/sec.	Slit width mm
130	169.5	rotated in air
212	346	rotated in air
273	532	rotated in air
580	990	rotated in air
475	1543	rotated in air
640	2500	rotated in air
754	3430	rotated in air
403	885	(in air)
682	2140	(in air)
1023	4810	(in air)
1330	4840	(in air)
1993	18750	(in air)
166	271	6.5 (in water)
220	428	6.5 (in water)
307	800	6.5 (in water)
390	1290	6.5 (in water)
463	1810	6.5 (in water)
573	2610	6.5 (in water)
784	5100	6.5 (in water)
403	885	6.5 (in water)
1265	8530	2.0 (in water)
519	467	(in air)
1111	2500	(in air)
598	1345	6.5 (in water)
617	1389	3.5 (in water)
654	1472	2.0 (in water)
617	1389	6.5 (in water)
529	953	6.5 (in water)
435	391	(in air)
817	1840	(in air)
226	203	3.5 (in water)
214	423	3.5 (in water)
460	1033	3.5 (in water)
741	3333	3.5 (in water)
926	6250	3.5 (in water)
1110	10000	

(in air), (in air), 3.5 (in water), 3.5 (in water), 3.5 (in water), 3.5 (in water), 3.5 (in water): length of inner cone 58 mm

Table VII

Influence of viscosity on power consumption (cone stirrer)

Speed r.p.m.	Power consumption in 10^{-4} N m/sec.	Viscosity in 10^{-3} N sec/m^2 (= c Poise)
161	72.5	(in air)
304	206	(in air)
420	377	(in air)
625	843	(in air)
942	2120	(in air)
1355	6100	(in air)
52½	236	480 (water glycerin dilutions)
109	981	
181	2440	
291	6550	
420	13200	
617	27800	
926	62500	
114	154	52
200	497	
345	1550	
467	3150	
604	5430	
794	10700	
1111	25000	
241	217	1
340	458	
515	1156	
855	3850	
1210	8150	
1390	12500	

Table VIII

Experimental results
Paddle stirrer (2 bl.)

Dimensions of stirrer d × w in 10^{-4} m^2	Volume of liquid V in 10^{-6} m^3	Vessel diam. D in 10^{-2} m	Liquid height H in 10^{-2} m	Stirrer speed n in rpm	Density difference $\Delta\rho$ in kg/m^3	Mixing time T in sec.	Dimensionless mixing time τ $\frac{Td^2wn}{V}$ (π^2 omitted)	Density Froude number $\frac{\rho n^2 d^2}{\Delta\rho gH}$	
6 × 1.2	2000	14.8	11.8	418	79.5	5.0	0.754	1.91	
				347		6.0	0.75	1.31	
				288		7.0	7.25	0.9	
				230		13.0	1.08	0.575	
				228		15.9	1.3	0.568	
				615		1.8	0.398	4.11	
				611	41.1	1.8	0.396	7.85	
				414		3.6	0.536	3.58	
				313		4.5	0.5	2.06	
				285		6.9	0.7	1.7	
				260	21.6	5.6	0.524	2.71	
				453		2.3	0.38	8.25	
				654		1.4	0.33	17.2	
				435	79.1	4.4	0.69	2.08	
				496		3.2	0.57	2.71	
				263	23.2	9.0	0.852	2.57	(exc.) e=0.5
				595		3.0	0.643	12.7	(exc.) e=0.5
4.5 × 1.2				260	21.6	13.1	0.685	1.52	
				598		4.4	0.533	8.05	
4.5 × 1.6				598	23.2	2.3	0.452	7.50	
				263		9.1	0.65	1.45	
3.37 × 1.2				275		19.5	0.75	0.89	
				600		5.0	0.408	4.22	
3.37 × 1.6				602		5.0	0.547	4.25	
				267		15.9	0.778	0.84	
5 × 2.0				260		7.1	0.78	1.75	
				259		6.0	0.65	1.75	
				598	21.1	2.0	0.498	9.4	
10.4 × 2.08				188	12	13.1	2.33	7.65	
	14000	26	26	187		13.0	0.651	3.45	
				144		23.0	0.887	2.05	
				320		5.4	0.463	10.1	
				421		3.2	0.361	17.5	
	10000	26	18.6	190		7.3	0.525	4.97	
	7000	21.5	21	188		9.9	1.0	4.63	
10.4 × 2.78	14000	26	26	345		3.2	0.394	11.0	
				340		4.8	0.591	11.4	
7.8 × 2.08	10000	26	18.6	184		11.5	0.465	2.62	
	14000	26	26	189		16.9	0.502	1.98	
				412		6.3	0.405	9.4	
15.2 × 3.04	45000	38	38	190	12	6.2	0.305	5.20	
				192		5.8	0.288	5.30	
				190		5.6	0.276	5.2	4 baffles
				323		3.2	0.268	15.0	
				139		10.6	0.382	2.78	
12.0 × 2.4	2000	14.8	11.8	263	21.9	4.8	3.64	10.8	
				187		8.4	4.45	5.54	
14.0 × 2.8				188		7.7	6.35	7.49	
10.4 × 2.08				188		9.0	3.17	4.17	
				263		5.4	2.66	8.15	
8.25 × 1.65				190		9.5	1.68	2.68	Reynolds'
				265		5.2	1.27	5.19	number
6 × 1.2				188		10.8	0.732	1.38	$\frac{nd^2}{\nu}$
				265		6.6	0.63	2.75	
8.25 × 1.65	7000			423	8.6	17.1	1.93	20	424
				423	10.9	16.3	1.84	15.8	474
				272	9.6	15.1	1.09	7.4	632
				423	10.3	8.0	0.9	15.6	1140
15.2 × 3.04	45000	38	38	188	9.6	14.4	0.702	8.51	695
				185	8.2	10.0	0.48	9.7	2820

Table IX

Paddle stirrer

(influence $\frac{w}{d}$, injection method)

Dimensions of stirrer d × w in 10^{-4} m^2	Volume of liquid V in 10^{-6} m^3	Vessel diam. D in 10^{-2} m	Liquid height H in 10^{-2} m	Stirrer speed in rpm	Mixing time T in sec.	Dimensionless mixing time τ $\frac{Tnd^2w}{V}$ (π^2 omitted)	Ratio $\frac{w}{d}$
6 × 6	2 000	14.8	11.8	207	2.2	0.82	1
6 × 6				141	3.7	0.93	1
6 × 4				207	2.5	0.62	0.67
6 × 4				141	4.8	0.63	0.67
6 × 3				206	2.9	0.54	0.5
6 × 3				140	4.5	0.56	0.5
6 × 2				209	3.9	0.50	0.33
6 × 2				140	6.0	0.51	0.33
6 × 1				207	5.2	0.33	0.17
6 × 1				140	14.3	0.60	0.17

Table X

Turbomixer (12 bl.)
$\beta = 46^{o}$, $\sin \beta = 0.72$

Dimensions of stirrer d × w in 10^{-4} m^2	Volume of liquid V in 10^{-6} m^3	Vessel diam. D in 10^{-2} m	Liquid height H in 10^{-2} m	Stirrer speed n in rpm	Density difference $\Delta\rho$ in kg/m^3	Mixing time T in sec.	Dimensionless mixing time τ $\frac{Tnd^2w \sin \beta}{V}$ (π^2 omitted)	Density Froude number $\frac{\rho n^2 d^2}{\Delta\rho g H}$	
10 × 1.4	7000	21	21	186	158	12.7	0.57	0.316	
				142		19.7	0.675	0.179	
				187	81.8	11.5	0.522	0.604	
				141		14.2	0.484	0.347	
				186	42.5	11.2	0.503	1.16	
				143		13.4	0.462	0.667	
				188	21.9	8.1	0.367	2.25	
				143		10.2	0.35	1.30	
				187	10.9	6.0	0.271	4.52	
				142		7.9	0.27	2.61	
				188		4.8	0.215	8.97	
				143		5.8	0.199	5.17	
				262	21.6	4.0	0.249	4.50	
				102		16.0	0.393	0.68	
				142	82.5	15.6	0.532	0.345	
				186	42.5	8.8	0.392	1.16	
	14000	26	26	145	22	11.4	0.5	1.01	
				189	22	9.2	0.51	1.70	
	7000	21	21	182	22	12.2	0.555	2.11	(e=0.5) exc.
	7000			143	22	15.2	0.533	1.31	„

Table XI

2-blade paddle stirrer with inclined blades ($\alpha = 40^{o}$)

Dimensions of stirrer $d \times w$ in 10^{-4} m^2	Volume of liquid V in 10^{-6} m^3	Vessel diam. D in 10^{-2} m	Liquid height H in 10^{-2} m	Stirrer speed n in rpm	Density difference $\Delta\rho$ in kg/m^3	Mixing time T in sec.	Dimensionless mixing time τ $\frac{Tnd^2w \sin {}^{k}\alpha}{V}$ (π^2 omitted)	Density Froude number $\frac{\rho n^2 d^2}{\Delta\rho gH}$	
5.7 × 0.85	2000	14.8	11.8	433	75.7	12.2	0.62	1.94	
$\alpha = 40^{o}$				624		7.4	0.53	4.03	
$\sin {}^{k}\alpha =$				331		20	0.77	1.14	
0.5				436		13.2	0.67	1.97	
(from fig.				266		24.6	0.76	0.73	
25)				266	39.5	22.6	0.70	1.4	
				434		11.0	0.56	3.73	
				627		5.8	0.42	7.8	
				332		18.2	0.70	2.28	
				225		40	1.04	1.0	
				435		11.0	0.56	3.75	
				438	20.4	8.0	0.41	7.4	
				632		4.2	0.31	15.3	
				334		12.0	0.47	4.28	
				229		19.0	0.55	2.01	
				436		6.8	0.35	7.3	Reynolds' number $\frac{nd^2}{\nu}$
				267		16.0	0.50	2.74	
				154		55.0	0.99	0.91	
	2000	14.8	11.8	435	39.5	14.2	0.70	3.75	
	2000	14.8	11.8	1018	39	9.1	1.06	21	620
				1022		6.8	0.81	21	800
				1022		4.3	0.50	21	3900
				1007		2.3	0.26	21	40500
3-blade paddle stirrer with inclined blades ($\alpha = 30^{o}$)									
5 × 0.75	2000	14.8	11.8	274	76	50	0.96	0.6	
$\alpha = 30^{o}$				600	76	8.0	0.53	2.9	
$\sin {}^{k}\alpha =$				604	10	4.6	0.22	21.9	
0.4				310	10	15.0	0.36	5.77	
(fig. 25)				430	39	5	0.56	2.85	$\alpha = 90^{o}$

Table XII

3-blade propepeller stirrer

Dimensions of stirrer d × p in 10^{-4} m^2	Volume of liquid V in 10^{-6} m^3	Vessel diam. D in 10^{-2} m	Liquid height H in 10^{-2} m	Stirrer speed n in rpm	Density difference $\Delta\rho$ in kg/m^3	Mixing time T in sec.	Dimensionless mixing time τ $\frac{Tnd^2p}{V}$	Density Froude number $\frac{\rho n^2 d^2}{\Delta\rho gH}$	
8 × 8	7000	21.5	20	425	40.4	12.6	6.52	2 60	
				270		22.2	7.30	1,ø5	
				428	21	10	5.22	5.06	Reynolds' number
				200		31	7.55	1.10	
				270	11.2	15.2	5.0	3.77	$\frac{nd^2}{\nu}$
	7000			428	10.4	90	47	16	195
				430	10.3	52.5	27.5	16	248
				429	8.7	40	21	19	327
				423	9.3	33	17	17.5	574
				271	9.9	40	13.3	6.7	460
				270	10.5	25.5	8.33	6.3	870
				425	11.0	14.0	7.23	15	1750
16 × 16	45000	38	38	322	11.8	27.3	13.4	21	357
				321	12.3	20	9.73	20.2	507
				327	8.6	18	8.94	28.5	592
				323	12.2	15.5	7.6	20.2	820
				235	9.9	30	10.7	13.1	685
				330	8.6	15.0	7.54	28.5	1480
				247	11.4	22.5	8.43	12.5	1480
				250	8.8	14.5	5.5	16.4	1845
				320	8.4	12.4	6.03	28.0	3640
				251	6.4	13.6	5.17	22.5	6170
				315	9.3	10.8	5.17	24.8	8130
				215	20	23.6	7.72	4.4	
				310	20.3	11.0	5.19	9.0	
				267	40	16.2	6.60	3.4	
				361	40	10.6	5.84	6.21	
				288	21.2	11.8	5.17	7.5	
				350	10.6	8.6	4.58	22.1	
				262	10.6	12.4	4.95	12.3	
				150	10.8	26.2	5.98	3.97	
				286	21.2	8.6	3.75	7.32	exc. (e=0.5)
				400	21	5.6	3.41	14.5	"
				515	21	4.6	3.61	24.2	"
				200	21	12.2	3.71	3.57	"
				146	21	8.4	1.87	1.91	"
				195	20.6	26.0	7.74	3.51	4 baffles
				300	21	11.0	5.03	8.31	"
				470	21	5.3	3.8	20.6	"
				600	21	3.8	3.46	32.7	"

Table XIII

2-blade paddle stirrer (influence of volume ratio)

Dimensions of stirrer d × w in 10^{-4} m^2	Upper layer in 10^{-6} m^3	Under layer in 10^{-6} m^3	Vessel diam. D in 10^{-2} m	Liquid height H in 10^{-2} m	Stirrer speed in rpm	Density difference $\Delta\rho$ in kg/m^3	Mixing time T in sec.
6 × 1	1900	100	14.8	11.8	338	0.046	5.2
	1800	200					6.8
	1500	500					7.6
	1000	1000					8.2
	500	1500					7.6
	200	1800					7.3

Table XIV

Power consumption
Paddle stirrer

Dimensions of stirrer d × w in 10^{-4} m^2	Vessel diameter in 10^{-2} m	Number of revolutions in rpm	Dimensionless power factor $\frac{P}{\rho n^3 d^5}$	Reynolds' number $\frac{nd^2}{\nu}$	Stirrer position
6 × 1.2	14.8	94	0.665	5 650	central
		126	0.625	7 575	"
		179	0.596	10 780	"
		258	0.530	15 510	"
		404	0.518	24 300	"
4.5 × 1.2		150	2.89	5 130	"
		403	2.36	13 800	"
4.5 × 1.6		129	2.41	4 410	"
		1840	1.54	62 900	"
3.37 × 1.2		252	3.15	4 640	"
		690	3.53	12 700	"
5 × 2.0		134	2.58	5 600	"
		367	1.82	15 340	"
10.4 × 2.78	26	161	1.64	29 080	"
		234	1.55	42 200	"
		320	1.76	57 800	"
		180	1.44	32 500	"
		262	1.35	47 300	"
		254	1.43	45 800	"
10.4 × 2.78	21.5	192	1.25	34 700	"
		242	1.27	43 700	"
10.4 × 2.78	14.8	107	0.808	19 300	"
		178	0.567	32 100	"
		218	0,586	39 400	"
7.8 × 2.78	26	218	3.67	22 300	"
		327	3.27	33 400	"
		449	3.46	45 700	"
		147.5	3.22	15 050	"
		251	2.76	25 600	"
6 × 1.2	14.8	108	0.9	6 500	eccentric
		217	0.891	13 020	(e = 0.5)
		764	0.77	45 900	"
4.5 × 1.2		358	3.43	12 300	"
		858	3.09	29 300	"

Table XIV (continued)

Dimensions of stirrer $d \times w$ in 10^{-4} m^2	Vessel diameter in 10^{-2} m	Number of revolutions in rpm	Dimensionless power factor $\frac{P}{\rho n^3 d^5}$	Reynolds' number $\frac{nd^2}{\nu}$	Stirrer position
4.5 × 1.6		302	5.01	10 340	(e = 0.5)
		698	4.37	23 900	"
3.37 × 1.2		249	3.28	4 580	"
		674	3.47	12 400	"
5 × 2		515	5.35	21 500	"
10.4 × 2.78	26	179	2.91	32 300	"
		253	2.89	45 600	"
7.8 × 2.78	26	195	4.59	19 090	"
		278	4.51	28 400	"
		388	4.66	39 600	"
15.2 × 3.04	38	146	0.615	56 300	central
		178	0.691	68 600	"
		190	0.691	73 200	"
		255	0.7	98 400	"
		260	0.662	100 500	"
		365	0.626	141 000	"
		139	0.925	53 600	eccentric
		190	0.988	73 300	"
		240	0.962	92 600	"
		320	1.149	123 500	"
		145	2.55	56 900	4 baffles
		190	2.64	73 300	"
		250	2.74	96 500	"
		320	2.61	123 500	"
		400	2.21	154 500	"

Table XV

Turbomixer

Dimensions of stirrer $d \times w$ in 10^{-4} m^2	Vessel diameter in 10^{-2} m	Number of revolutions in rpm	Dimensionless power factor $\frac{P}{\rho n^3 d^5}$	Reynolds' number $\frac{nd^2}{\nu}$
10 × 1.4	21.5	295	1.015	49 300
		205	1.094	34 200
		126	1.16	21 000
		85.5	1.25	14 300

Table XVa

Paddle stirrer with varying vane angle β

Dimensions of stirrer $d \times w$ in 10^{-4} m^2	Vessel diameter in 10^{-2} m	Number of revolutions in rpm	Dimensionless power factor $\frac{P}{\rho n^3 d^5}$	Reynolds' number $\frac{nd^2}{\nu}$	Vane angle β	sin β
6 × 1.2	14.8	284	1.52	11 400	30°	0.5
		209	1.44	8 350		
		172	1.32	8 350	45°	0.707
		235	1.37	11 400		
		213	1.21	12 000	60°	0.866
		277	1.49	15 500		
		183	1.41	11 000	90°	1
		281	1.33	16 900		

STELLINGEN

1. De door SMIRNOV en POLYNTA gevolgde procedure om, met behulp van dimensie-analyse een formule af te leiden voor de diameter van een uit een pipet uitstromende druppel, is in principe onjuist.

   N.I.Smirnov, S.F.Polynta, Zhur.Priklad Khim. **21** 1137, 1948.

2. De uitspraak van LARCOMBE betreffende de invloed van de dichtheid op de druppeldiameter bij verstuiving is in tegenspraak met die van andere onderzoekers.

   H.G.Houghton, Perry, Chem.Eng.Handbook, 3rd ed., 1950, p.1174.
   J.Larcombe, The Chemical Age, p.563, 596, 621, 1947.

3. Wanneer menging in een vat moet worden verkregen door injectie van een vloeistofstraal, welke via een mondstuk aan het eind van een lange leiding met constant drukverschil uitstroomt, dan verdient het aanbeveling de uitstroom-opening zo te dimensioneren, dat de impuls van de uittredende stroom per tijdseenheid maximaal is.

4. De invloed van de roercondities op de emulgering in een geroerd vat wordt voornamelijk bepaald door de grootte van de turbulente energie-toevoer per volume-eenheid.

5. De moeilijkheid, welke HIXSON en SMITH ondervonden bij het correleren van hun resultaten over de extractiesnelheid bij geroerde emulsies, zijn waarschijnlijk te wijten aan onvoldoende dispergering gedurende het experiment.

   A.W.Hixson, M.I.Smith, Ind.Eng.Chem. **41** 973, 1949.

6. Bij het uitwassen van filterkoeken verbetert de vorm der wascurve als de zijdelingse (radiale) menging toeneemt.

7. De verschillen in bezinkingssnelheid bij een al of niet geroerd „particulate fluid bed" kunnen met behulp van het classificatieverschijnsel worden verklaard.

   R.Jottrand J.of Appl.Chem. **2** S 17, 1952.

8. Als een fijnverdeelde vaste stof aan een emulsie wordt toegevoegd, is er een neiging dat die fase continu wordt, die met die vaste stof de kleinste randhoek vormt.

9. De ongunstige invloed van „backmixing" van de continue fase op het extractieresultaat bij tegenstroomextractie is minder groot wanneer het oplosmiddel dispers is, dan wanneer het oplosmiddel continu is.

10. Bij hun berekeningen over het „flooding" verschijnsel in gepakte extractie-kolommen, gaan PRATT en medewerkers er ten onrechte van uit, dat beide vloeistoffasen continu zijn.

    F.R.Dell en H.R.C.Pratt. Trans.Inst.Chem.Eng. **29** 84 e.v., 1951.

11. De invloed van factoren als leeftijd en levensomstandigheden op de afmetingen en de verhouding der afmetingen van de anadonta cygnea (zwanemossel) is zodanig, dat het toepassen van deze afmetingen als systematisch kenmerk onaanvaardbaar moet worden geacht.

    V.Franz, Jenaische Zeitschr.f.Nat.Wissensch. **72** 75, 1939. Tera van Benthem Jutting „Fauna van Nederland", Leiden 1943, p.133.

12. De uitspraak van GAUTIER over VILLON: „S'il avait employé au bien tout l'esprit et tout le génie qu'il dépensa au mal, nous aurions peut-être perdu le poête, en gagnant l'honnête homme", wordt discutabel, indien men alleen het latere oeuvre van VILLON beoordeelt.

    Théophile Gautier, „Les Grotesques", Paris, 1914.

13. Het is onjuist om, zoals Italo Siciliano doet, de romantiek (in de literatuur) te beschouwen als een renaissance van de Middeleeuwen.

    Italo Siciliano: „François Villon et les Thèmes poétiques du Moyen Age", Paris 1934, p.527-551.